nurix

Leader in Targeted Protein Modulation

NX-1607: a First-In-Class Inhibitor of Casitas B-lineage Lymphoma B (CBL-B) for Immuno-Oncology

Frederick Cohen, Paul Barsanti, Neil Bence, Alexandra Borodovsky, Brandon Bravo, Jilliane Bruffey, Mario Cardozo, Ming Liang Chan, Ganesh Cherala, Matthew Clifton, Thomas Cummins, Ketki Dhamnaskar, Stefan Gajewski, Marilena Gallotta, Jose Gomez-Romo, Jennifa Gosling, Cristiana Guiducci, Gwenn M Hansen, Joseph Juan, Christopher Karim, Dane Karr, Kathrine Kurylo, Mitchell Lavarias, Morgan Lawrenz, Jenny McKinnell, Jeff Mihalic, Ratul Mukerji, Nichole O'Connell, Janine Powers, Serena Ranucci, Ryan Rountree, Anjanabha Saha, Arthur T Sands, Julie Sheung, Hunter Shunatona, Jennifer Stokes, Asad Taherboy, Ying Siow Tan, Hiroko Tanaka, Austin Tenn-McClellan, Jennifer Tung, Chenbo Wang, Dahlia Weiss, Christoph Zapf

Drug Discovery Chemistry, San Diego, April 02, 2024

Important Notice and Disclaimers

This presentation contains statements that relate to future events and expectations and as such constitute forward-looking statements within the meaning of the Private Securities Litigation Reform Act of 1995. When or if used in this presentation, the words “anticipate,” “believe,” “could,” “estimate,” “expect,” “intend,” “may,” “outlook,” “plan,” “predict,” “should,” “will,” and similar expressions and their variants, as they relate to Nurix Therapeutics, Inc. (“Nurix”, the “Company,” “we,” “us” or “our”), may identify forward-looking statements. All statements that reflect Nurix’s expectations, assumptions or projections about the future, other than statements of historical fact, are forward-looking statements, including, without limitation, statements regarding our future financial or business plans; our future performance, prospects and strategies; future conditions, trends, and other financial and business matters; our current and prospective drug candidates; the planned timing and conduct of the clinical trial programs for our drug candidates; the planned timing for the provision of updates and initial findings from our clinical studies; the potential advantages of our DELigase™ platform and drug candidates; the extent to which our scientific approach and DELigase™ platform may potentially address a broad range of diseases; the extent animal model data predicts human efficacy; and the timing and success of the development and commercialization of our current and anticipated drug candidates. Forward-looking statements reflect Nurix’s current beliefs, expectations, and assumptions. Although Nurix believes the expectations and assumptions reflected in such forward-looking statements are reasonable, Nurix can give no assurance that they will prove to be correct. Forward-looking statements are not guarantees of future performance and are subject to risks, uncertainties and changes in circumstances that are difficult to predict, which could cause Nurix’s actual activities and results to differ materially from those expressed in any forward-looking statement. Such risks and uncertainties include, but are not limited to: (i) risks and uncertainties related to Nurix’s ability to advance its drug candidates, obtain regulatory approval of and ultimately commercialize its drug candidates; (ii) the timing and results of clinical trials; (iii) Nurix’s ability to fund development activities and achieve development goals; (iv) the impact of macroeconomic conditions, including inflation, increasing interest rates and volatile market conditions, and global or regional events, including regional conflicts, on Nurix’s clinical trials and operations; (v) Nurix’s ability to protect intellectual property and (vi) other risks and uncertainties described under the heading “Risk Factors” in Nurix’s Annual Report on Form 10-K for the fiscal year ended November 30, 2023, and other SEC filings. Accordingly, readers are cautioned not to place undue reliance on these forward-looking statements. The statements in this presentation speak only as of the date of this presentation, even if subsequently made available by Nurix on its website or otherwise. Nurix disclaims any intention or obligation to update publicly any forward-looking statements, whether in response to new information, future events, or otherwise, except as required by applicable law.

Certain information contained in this presentation relates to or is based on studies, publications, surveys and other data obtained from third-party sources and the Company’s own internal estimates and research. While the Company believes these third-party sources to be reliable as of the date of this presentation, it has not independently verified, and makes no representation as to the adequacy, fairness, accuracy or completeness of, any information obtained from third-party sources. In addition, all of the market data included in this presentation involves a number of assumptions and limitations, and there can be no guarantee as to the accuracy or reliability of such assumptions. Finally, while we believe our own internal estimates and research are reliable, such estimates and research have not been verified by any independent source

CBL-B Is a Modulator of Immune Cell Activation

- CBL-B is an E3 ubiquitin ligase highly expressed in cells of the immune system
- CBL-B regulates T, B, and NK cell activation
- Blocking CBL-B removes a brake on the immune system
- *cbl-b* deficient mice demonstrate robust T-cell and NK cell-mediated antitumor immunity

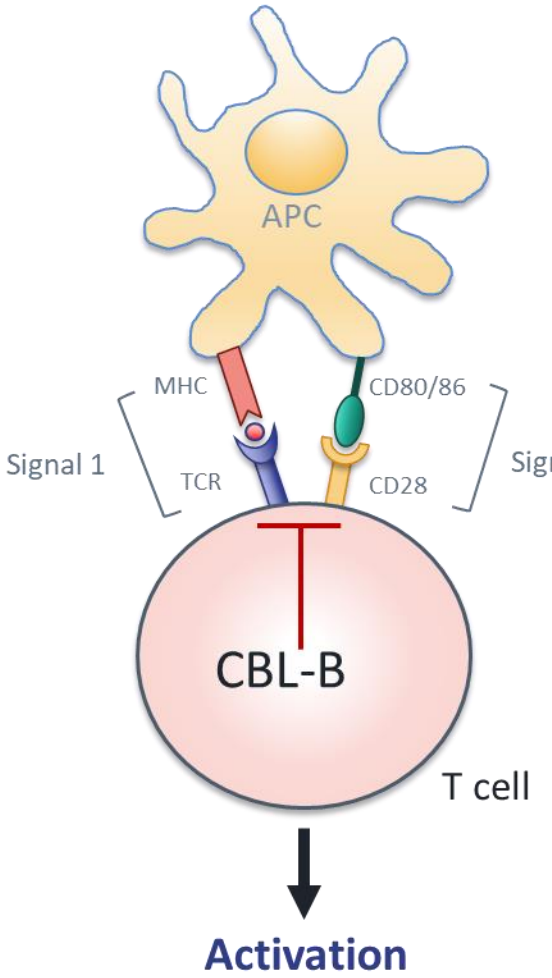

CBL-B inhibition

- IL-2 production
- Proliferation
- Central memory phenotype
- Anti-tumor activity
- Threshold of activation
- T-cell exhaustion

Synergy with anti-PD-1

Loss of CBL-B Activity Results in Enhanced T-cell Activation

KO and ligase inactive (KI) T-cells exhibit increased IL-2 secretion upon *ex vivo* stimulation

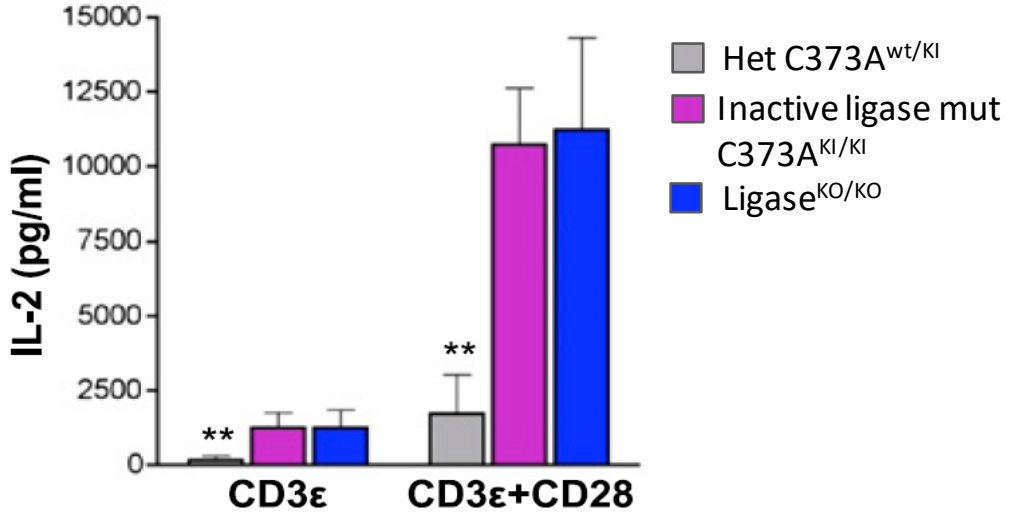

Paolino et. al. *J. Immunology*, 2011

Ligase-dead or KO exhibit enhanced and equivalent response to either single or double stimulation

Ligase-inactive *cbl-b* knock-in mice exhibit tumor growth inhibition (TC-1 syngeneic model)

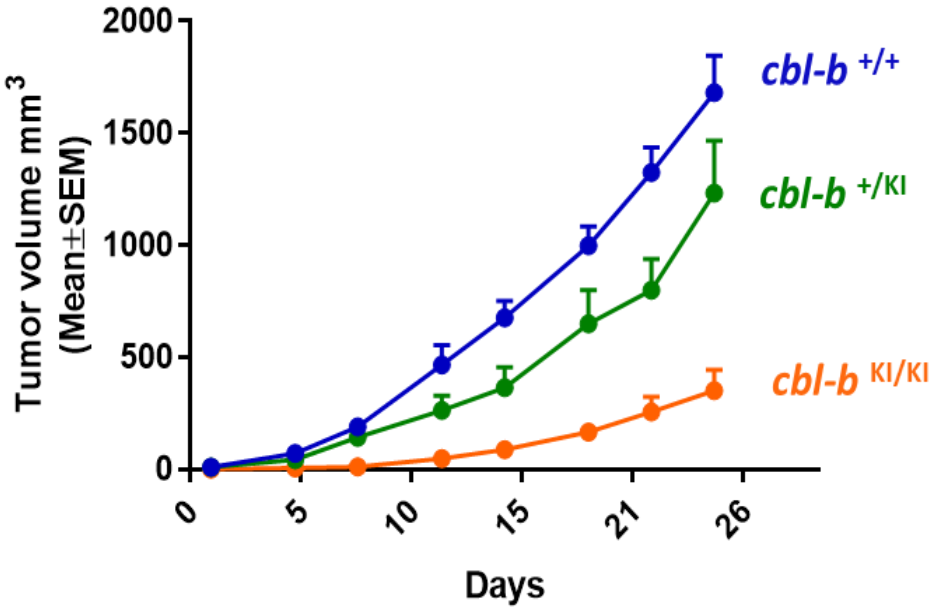

Unpublished Data

Activation of CBL-B Requires Phosphorylation

"Closed-state" (inactive)

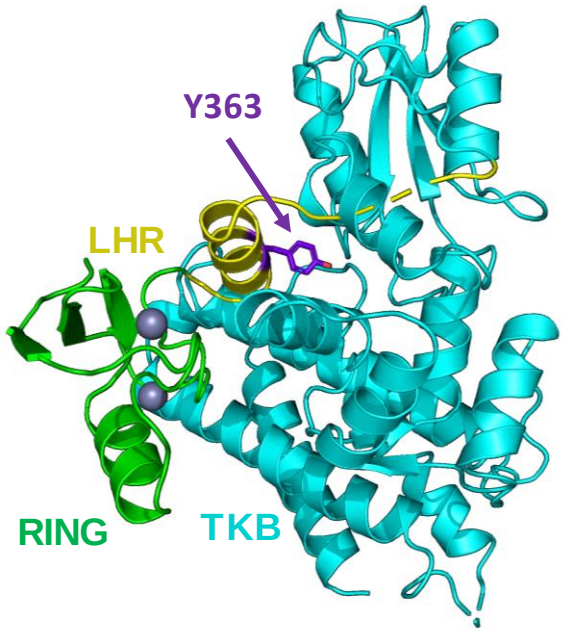

PDB: 8ULI

Phosphorylation

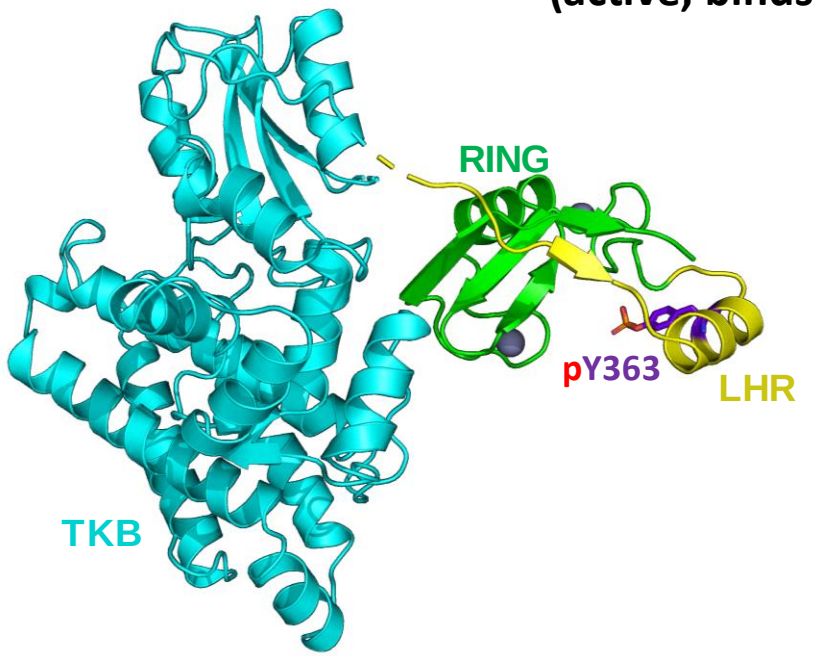

"Open-state" (active, binds E2-Ub)

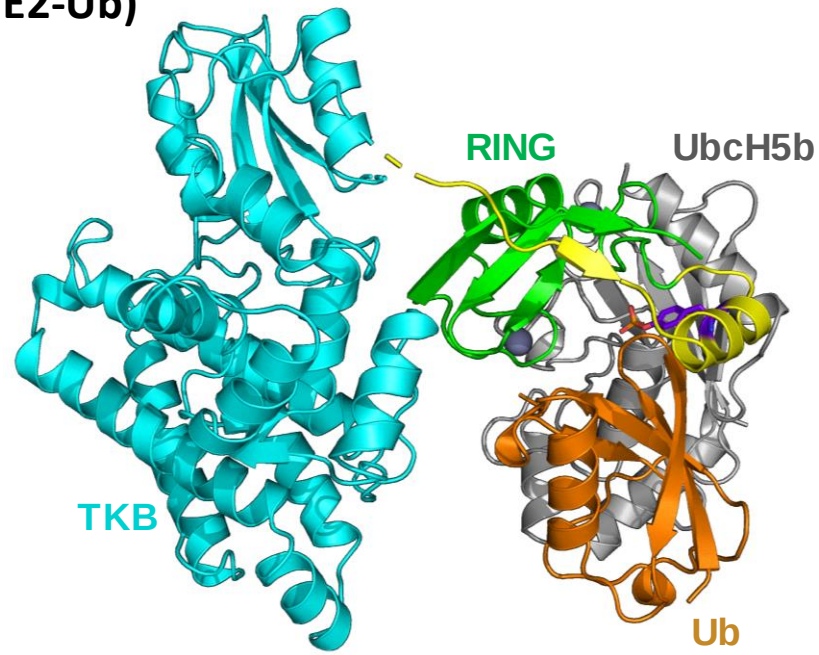

PDB: 3NZI

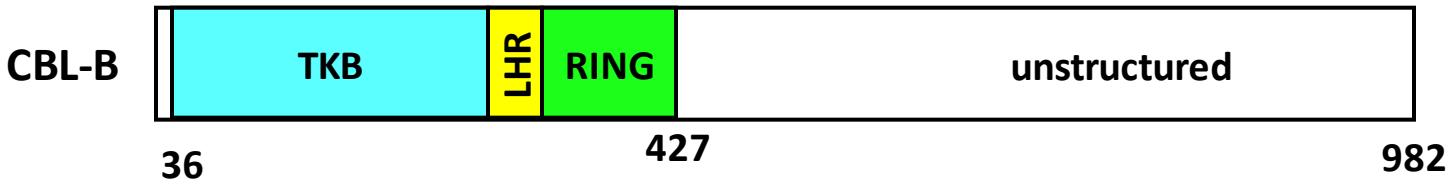

NRX-3 Is a Specific, Intramolecular Glue Inhibitor of CBL-B

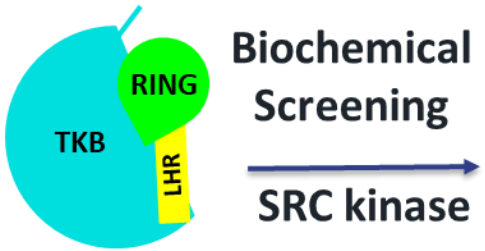

SRC counter-screen

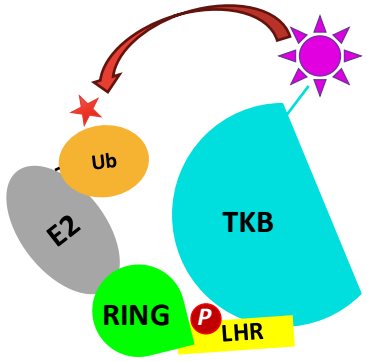

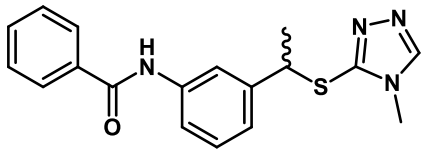

NRX-1
Singleton hit from 300K HTS screen

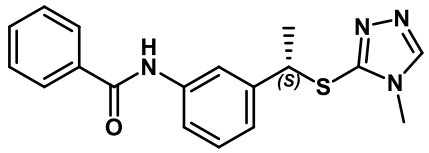

NRX-3
Resolved Screening hit
mw = 338; LE = 0.29

E2-Ub Binding Assay

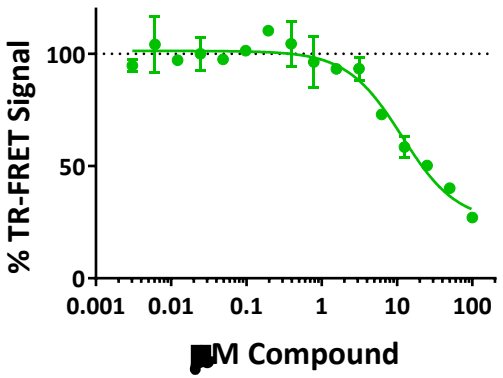

IC_{50} = 12 µM

SPR

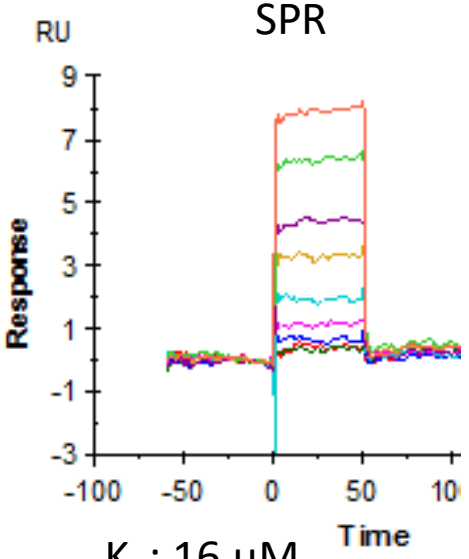

K_D: 16 µM

NRX-3 Is a Specific, Intramolecular Glue Inhibitor of CBL-B

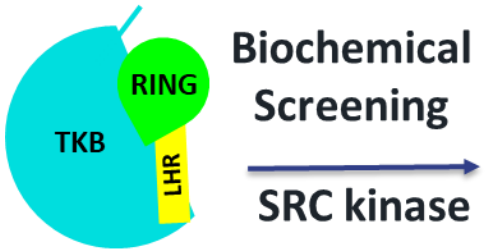

Biochemical Screening

SRC kinase

SRC counter-screen

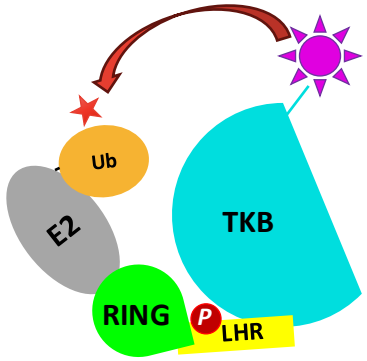

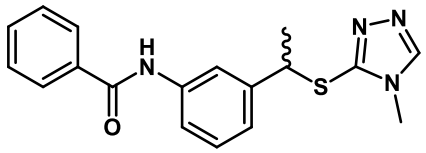

NRX-1
Singleton hit from 300K HTS screen

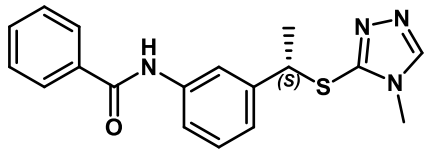

NRX-3
Resolved Screening hit
mw = 338; LE = 0.29

E2-Ub Binding Assay

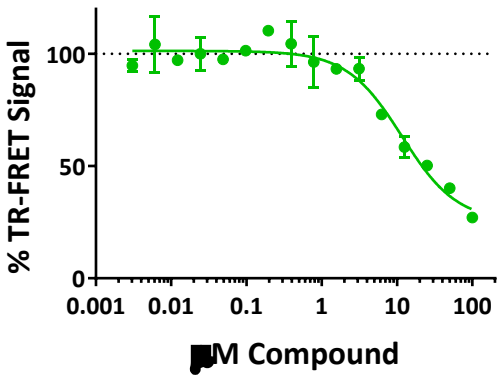

IC_{50} = 12 µM

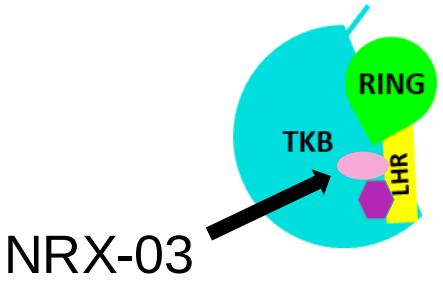

NRX-03

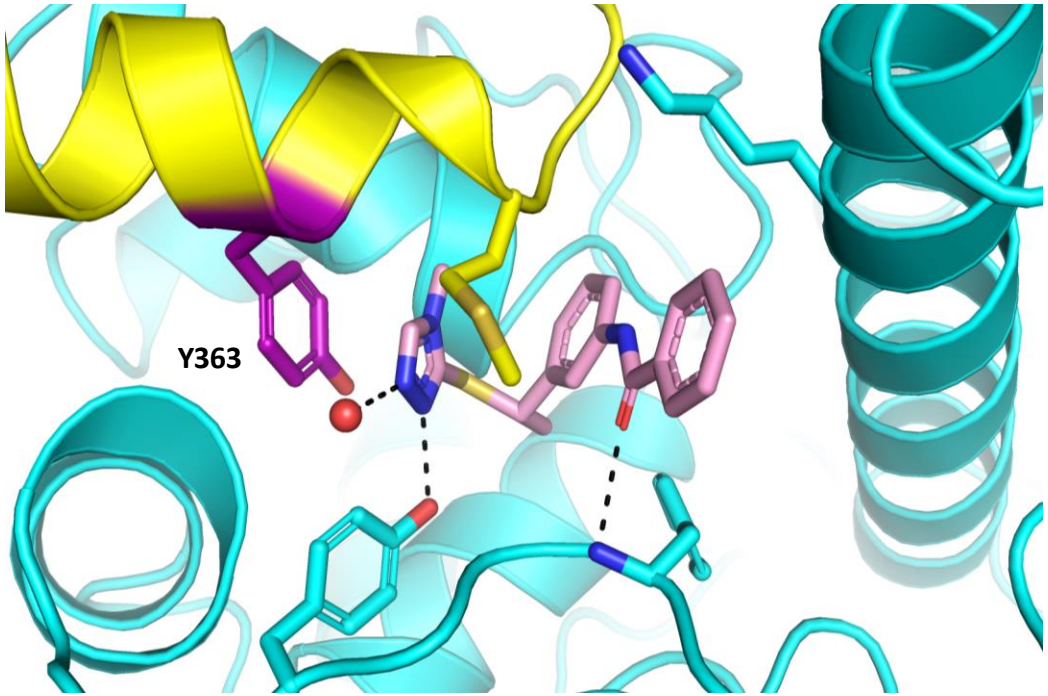

SPR

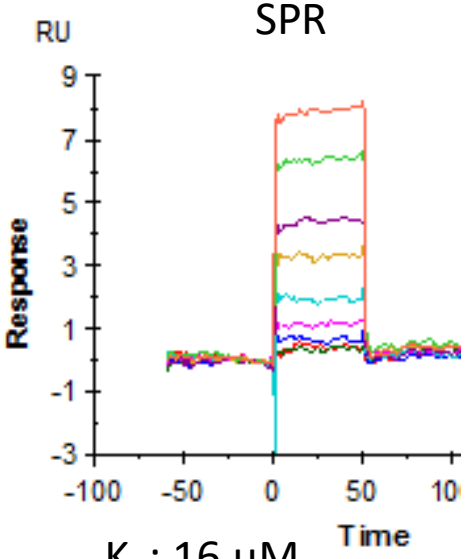

K_D: 16 µM

nurix

Testing Funnel Designed To Identify Optimal T-cell Activators

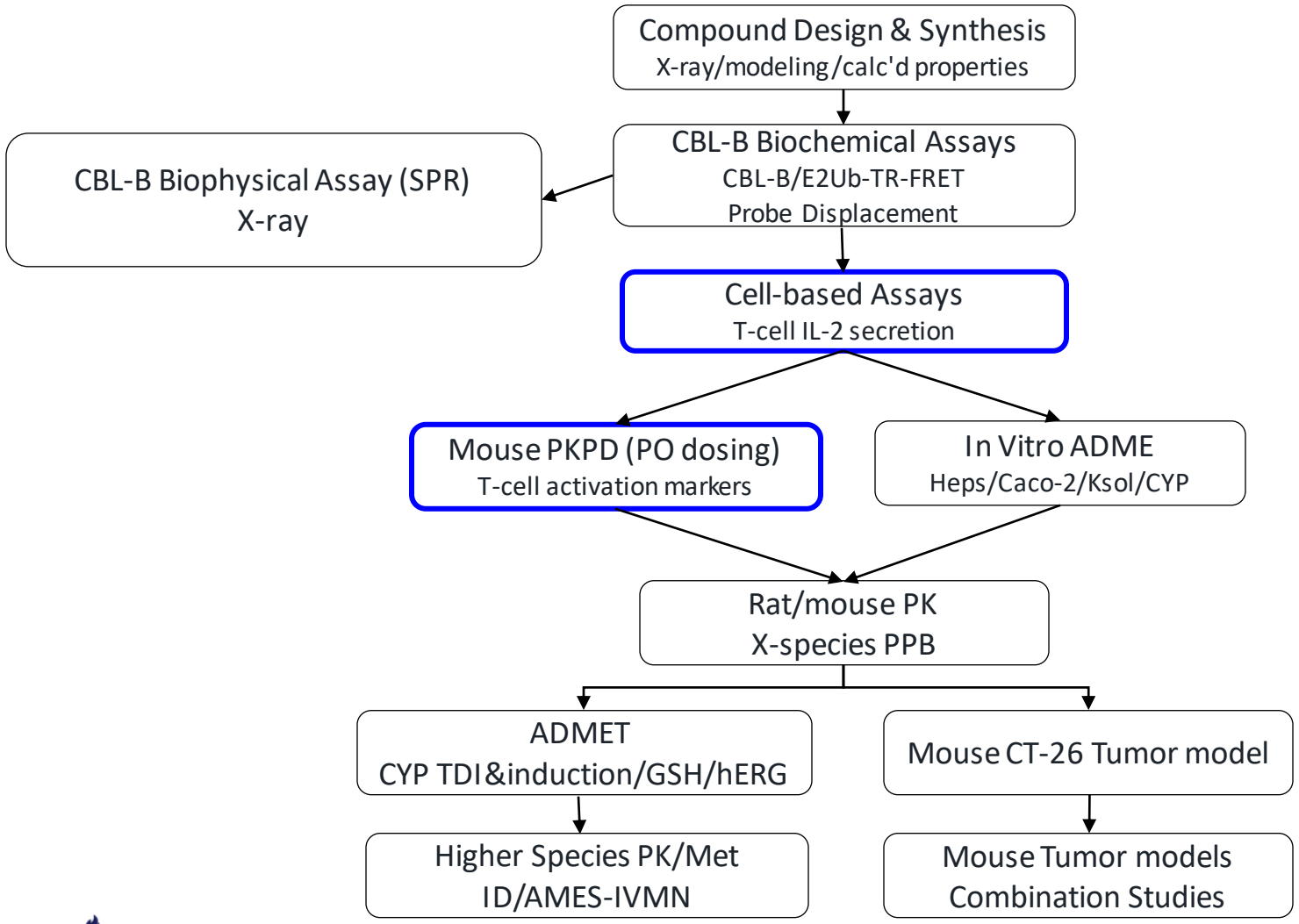

- T-cell activation assays (*in vitro/vivo*) were primary drivers of optimization
- *In vitro* ADMET was collected in parallel with *in vivo* assays

Cytokine Release Assay for T-cell Activation

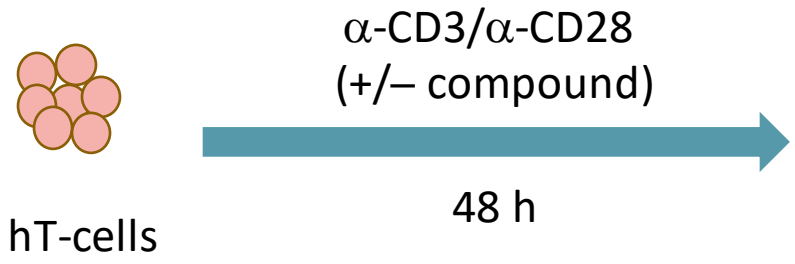

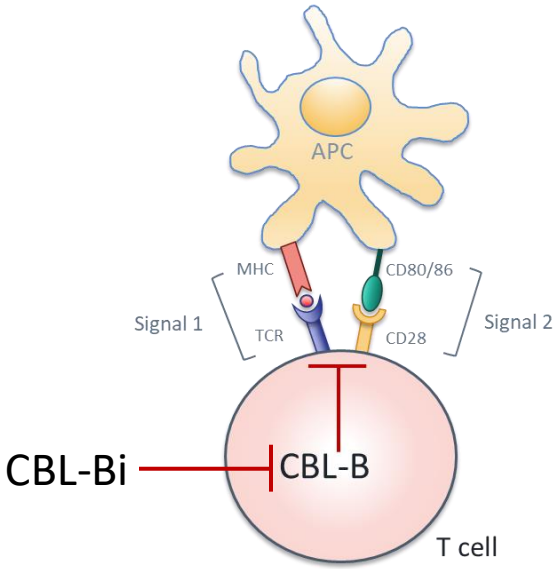

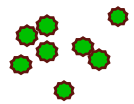

Cytokine Production

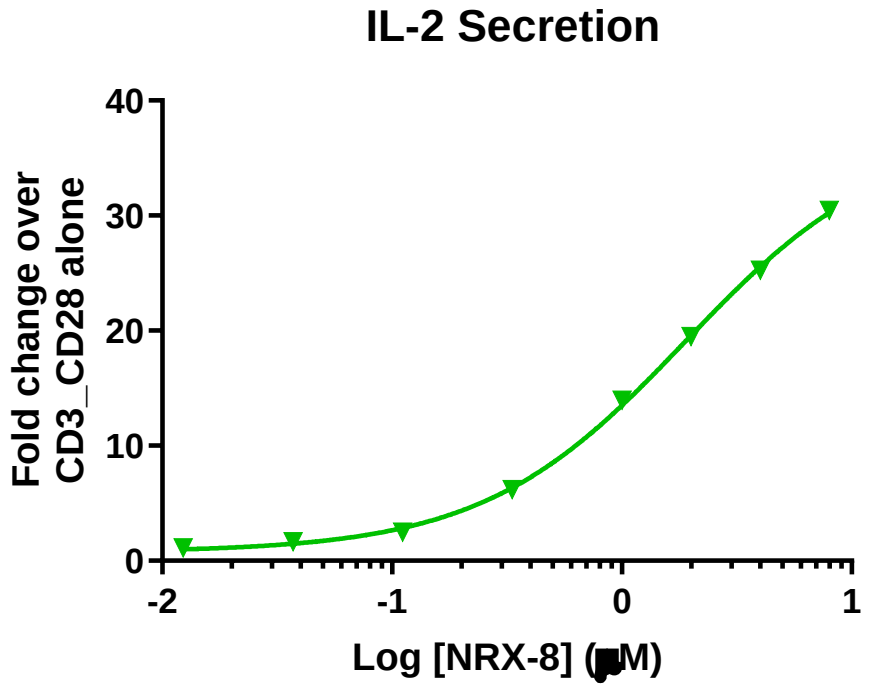

Cytokine Release Assay for T-cell Activation

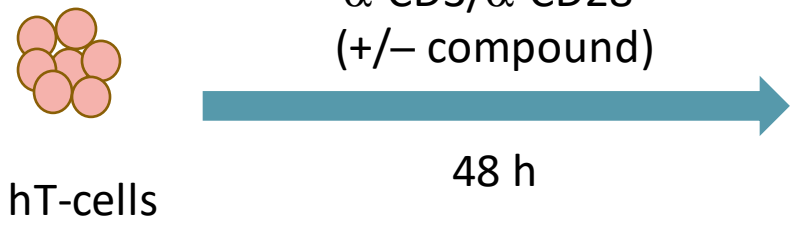

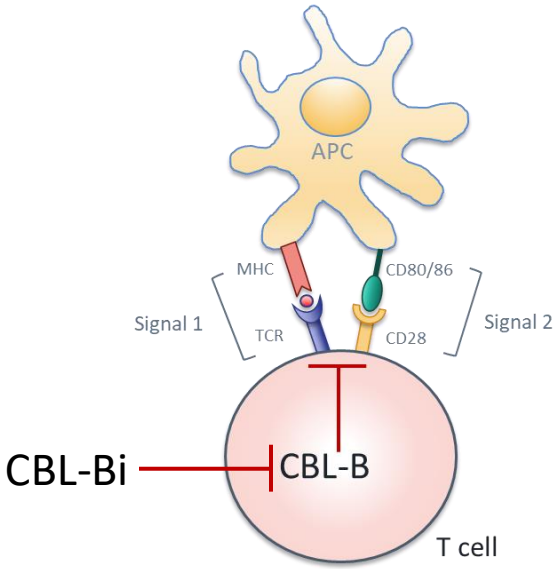

Cytokine Production

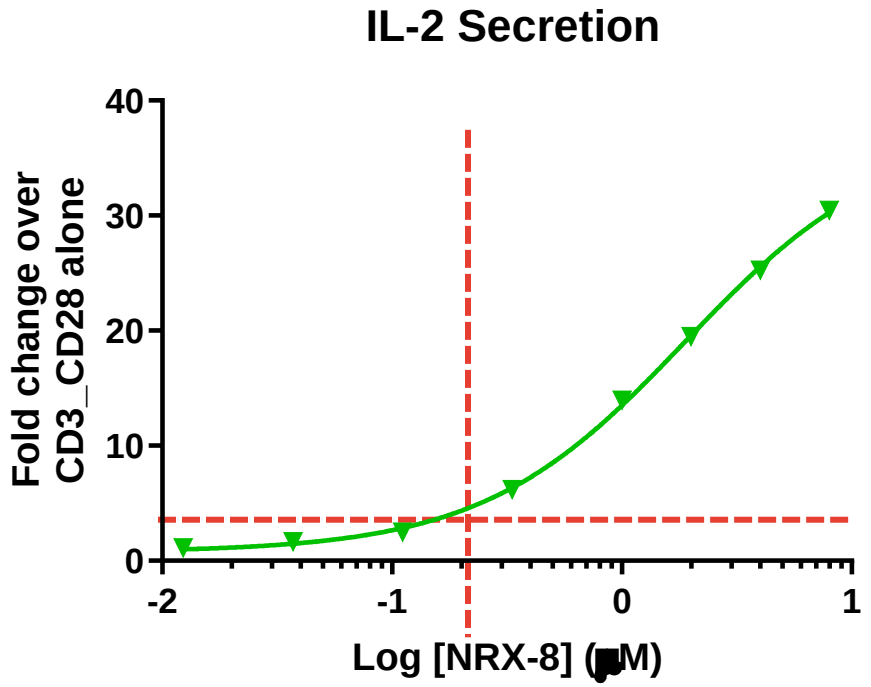

2.5-fold induction

Concentration for Threshold

Mouse PK/PD Assay for T-cell Activation

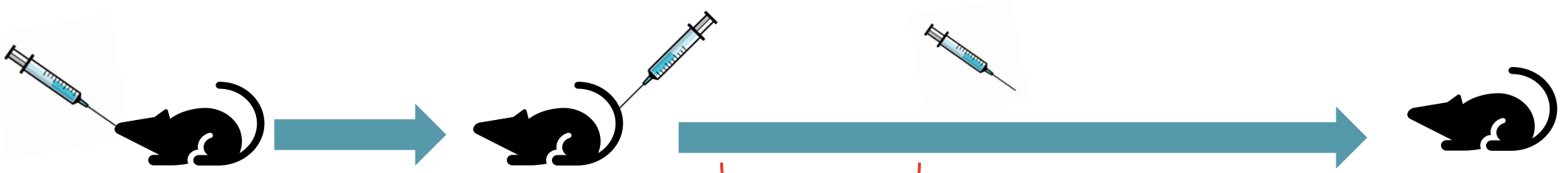

- T_{0h}
- CBL-Bi PO

- $T_{0.25h}$
- Anti-CD3
- (2μg) IV

PK samples

- T_{8h}
- CBL-Bi PO

- T_{24h}
- Analysis of splenic T-cells by flow

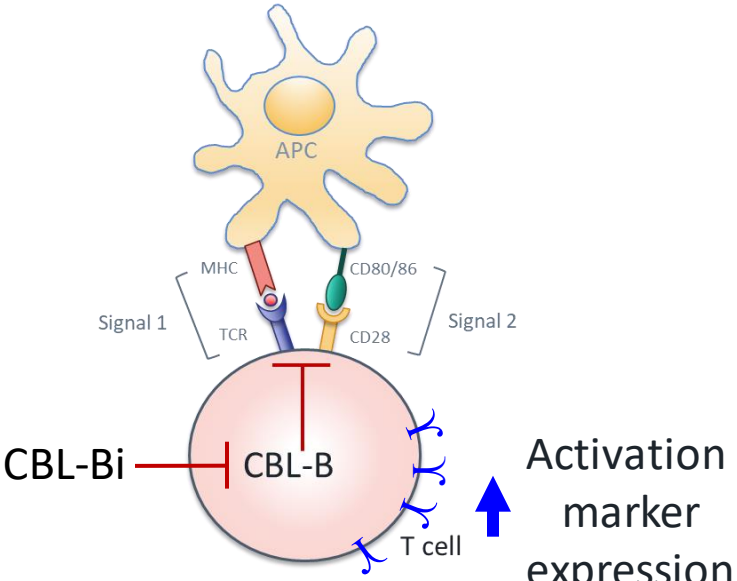

Activation marker expression

Activation marker expression level in T-cells:

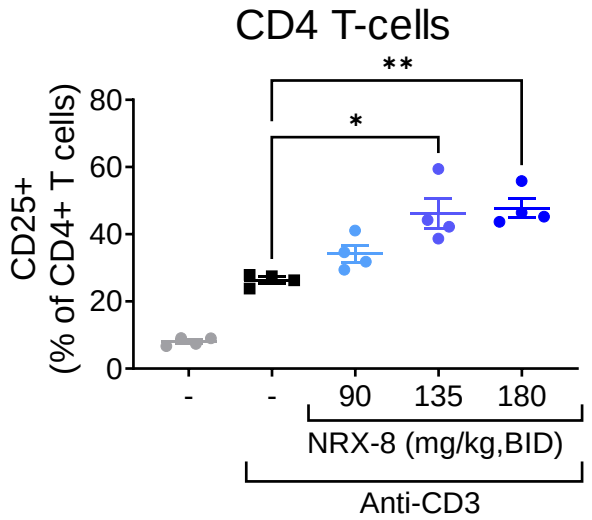

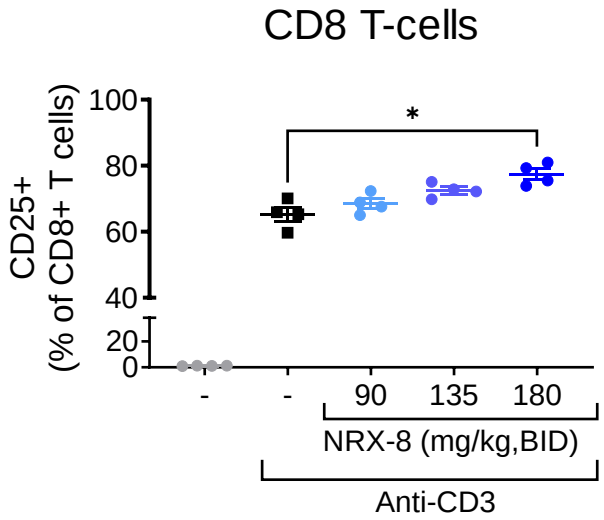

Amide Series Provided Early POC

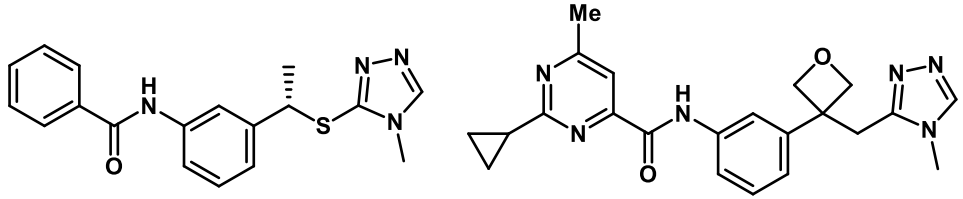

	NRX-3	NRX-8
CBL-B E2-Ub: IC_{50} (μM)	12	0.021
T-cell IL-2 AUC		29
T-cell IL-2 2.5X (μM)		0.1
Hep Stability h/m (pred CL hep, ml/min/kg)		<1/34
Plasma stability m/r $T_{1/2}$ (min)		>1000/>1000
Dose mg/kd; freq		180/BID
Free Conc 2h/6h (μM)		1.8/-
Fold increase CD25+/CD4+ cells (24h)		2.1

First confirmation that CBL-B inhibition reproduces the genetic phenotype.

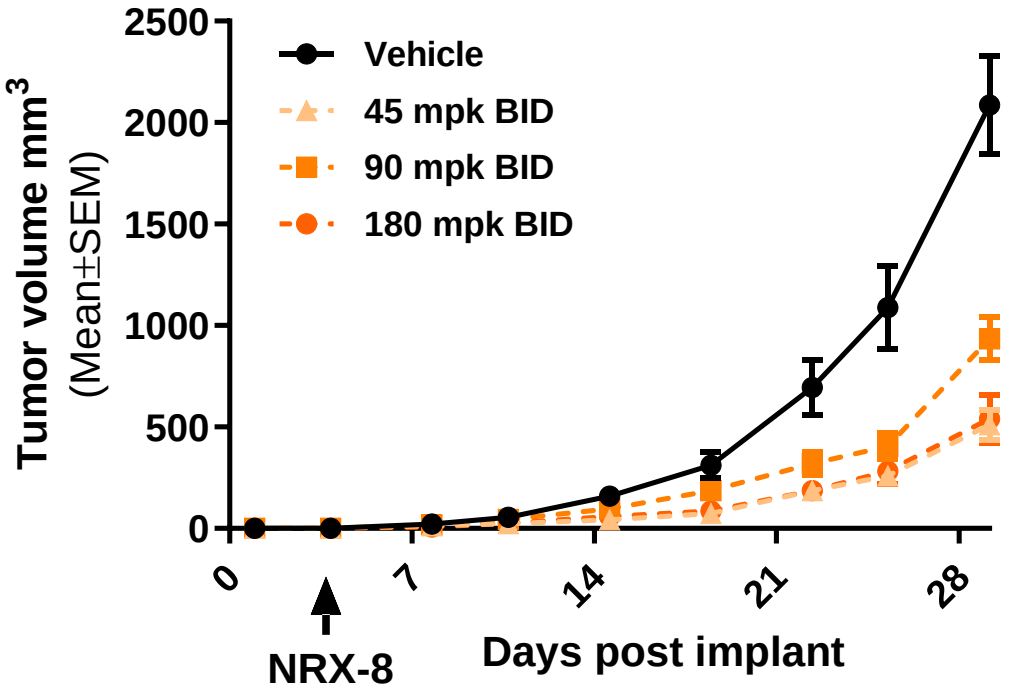

CT26 Syngeneic Model

Sources: 1) AACR, 2019 abstract 2610 2) "Discovery and Optimization of CBL-B Inhibitors" ACS Fall meeting 2022

Cyclizing the Amide Solves the Variable Plasma Stability Problem

R = 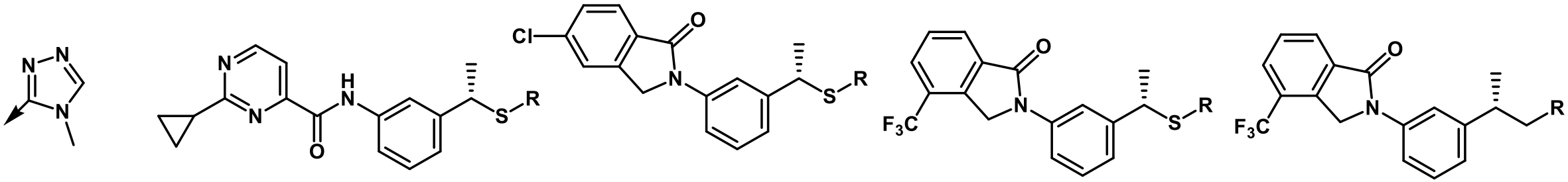

	NRX-5	NRX-9	NRX-10	NRX-11
CBL-B E2-Ub: IC_{50} (μM)	**0.092**	**0.62**	**0.18**	**0.059**
Hep Stability h/m (pred CL hep, ml/min/kg)				**15/77**
Plasma stability m/r $T_{1/2}$ (min)	**140/-**			**>1000/>1000**

1,2,4-Triazole is the Optimal Heterocycle for CBL-B Affinity

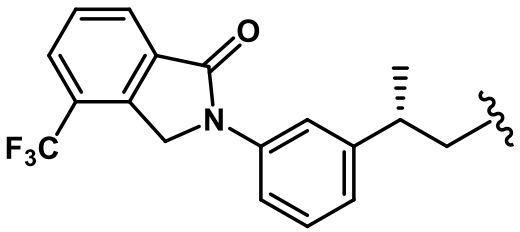

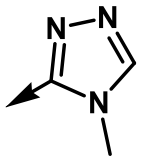

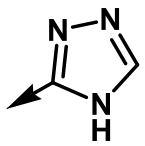

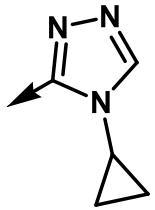

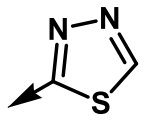

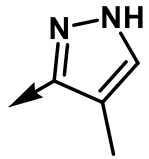

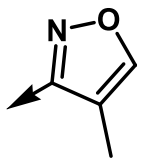

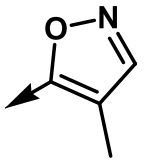

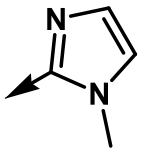

	NRX- 11	NRX-12	NRX-13	NRX-14	NRX-15	NRX-16	NRX-17	NRX-18
CBL-B E2-Ub: IC_{50} (μM)	0.059	0.34	0.74	0.72	0.51	0.35	2.7	30

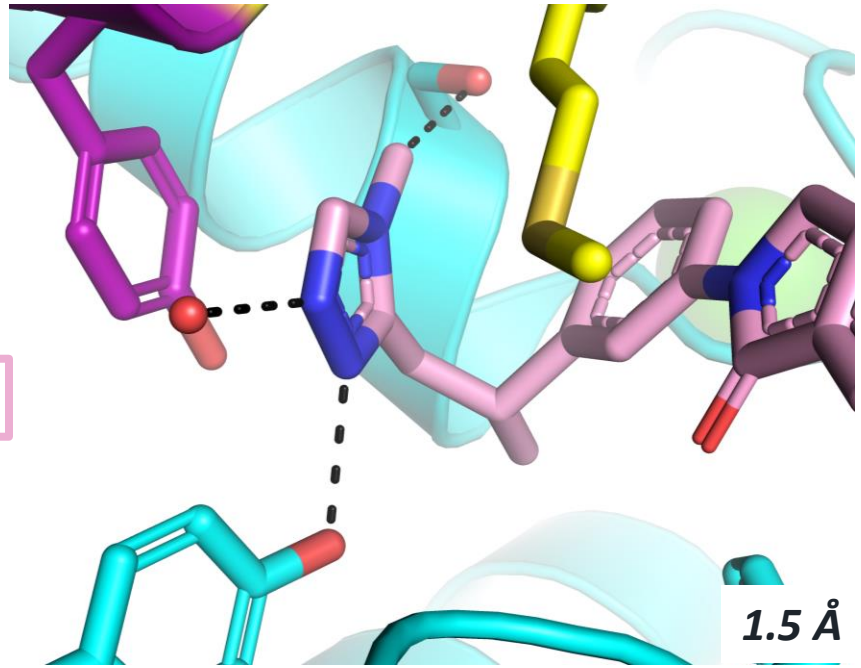

- Two H-bond acceptors required for affinity
- N-Methyl is the optimal ring substituent for affinity

Spacer SAR for Affinity and Metabolic Stability

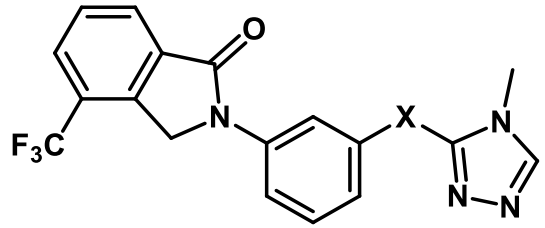

X =

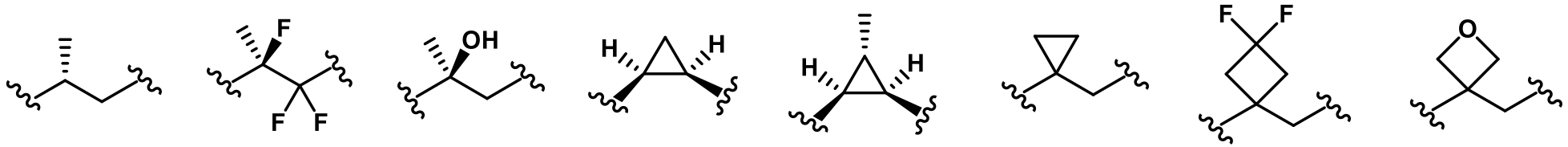

	NRX-11	NRX-19	NRX-20	NRX-21	NRX-22	NRX-23	NRX-24	NRX-25
CBL-B E2-Ub IC_{50} (μM)	0.059	0.15	6.9	0.33	0.039	0.045	0.025	0.067
T-cell IL-2 2.5x (μM)	1.5	0.44	-	2.2	0.21	0.34	0.13	2.5
Hep Stability h/m (pred CL hep, ml/min/kg)	15/76	<8/35	<8/<28	<8/50	<8/79	17/80	15/17	<8/<28

Spacer SAR for Affinity and Metabolic Stability

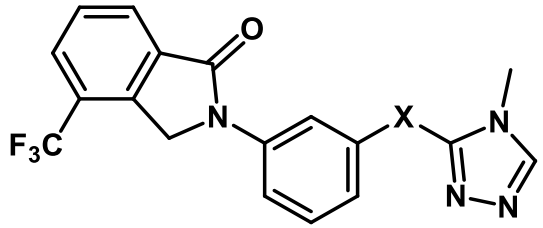

X =

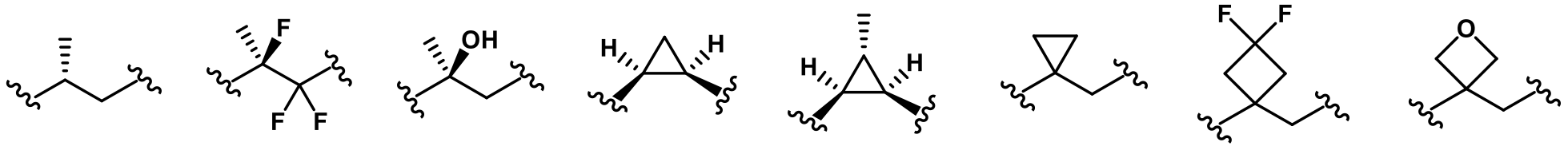

	NRX-11	NRX-19	NRX-20	NRX-21	NRX-22	NRX-23	NRX-24	NRX-25
CBL-B E2-Ub IC_{50} (μM)	0.056	0.15	6.9	0.33	0.039	0.045	0.025	0.067
T-cell IL-2 2.5x (μM)	1.5	0.44	-	2.2	0.21	0.34	0.13	2.5
Hep Stability h/m (pred CL hep, ml/min/kg)	15/76	1.7/35	<8/<28	<8/50	<8/79			<8/<28
Mouse PKPD: Dose mg/kd; freq	180; BID#			180;BID#	#BID doses at T 0, 8h			
Mouse PKPD: Free Conc 2h/6h (μM)	0.44/0.11			4.3/2.6				
Mouse PKPD: Fold increase CD25+/CD4 + cells (24h)	2.3			2.6				

Co-Crystal Structures Suggest a New Pocket for Affinity

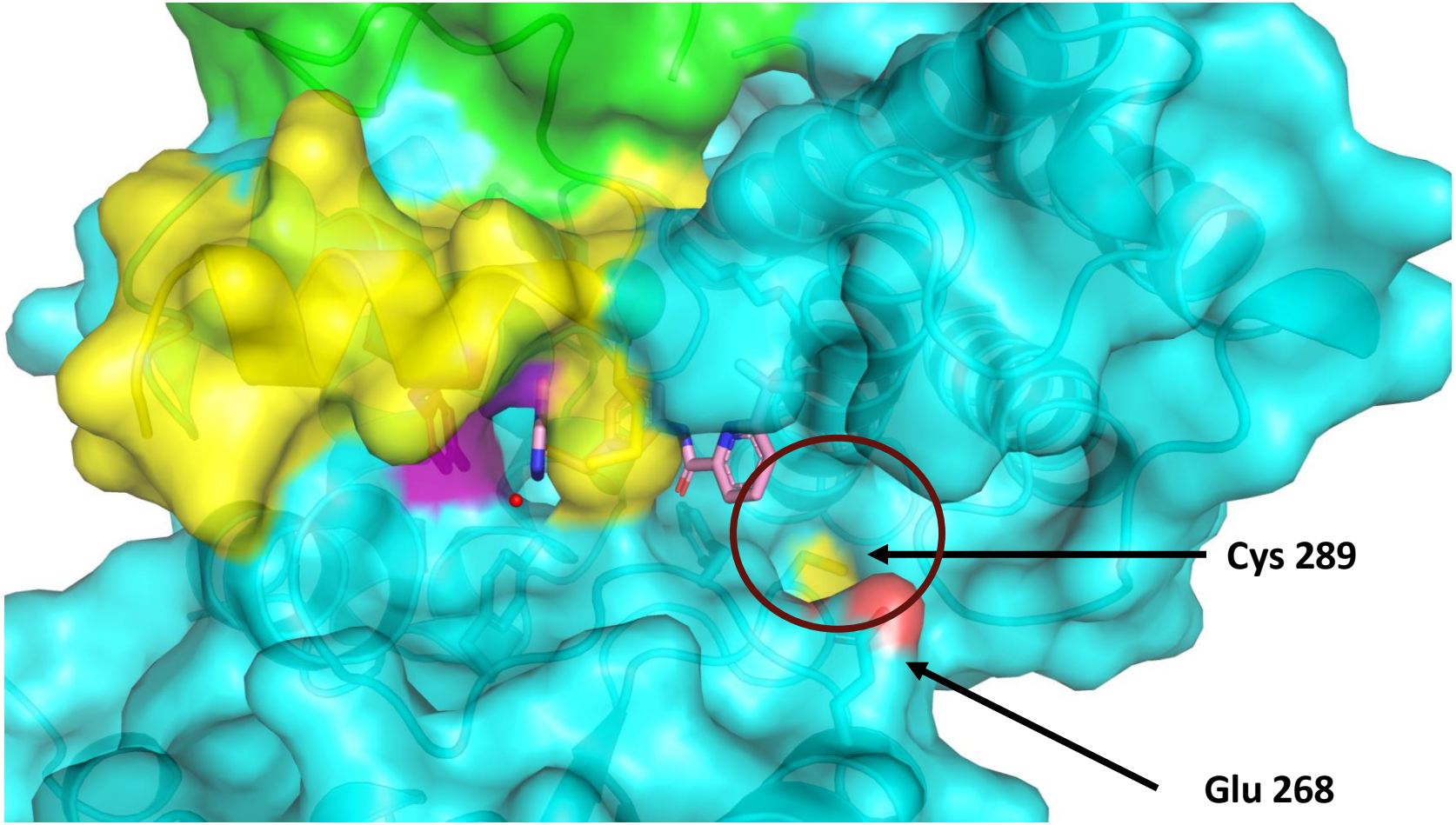

Piperidines and Pyrrolidines Optimally Fill the New Pocket

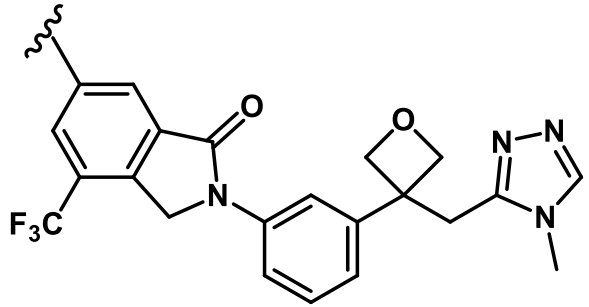

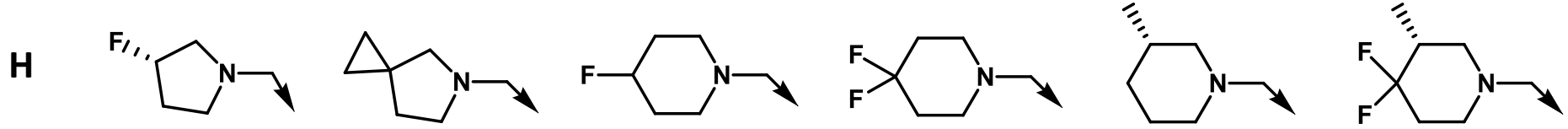

	NRX-25	NRX-26	NRX-27	NRX-28	NRX-29	NRX-30	NRX-31
CBL-B E2-Ub IC_{50} (nM)	150	5.1	5.1	4.8	6.2	8.8	4.9
TR-FRET Probe Displacement (nM)		9.1	4.2	4.7	8.6	2.0	1.6
T-cell IL-2 AUC		32.2	38	43.1	39	23.4	54
T-cell IL-2 2.5x (nM)	2500	72.1	6.4	12.8	17.6	6.3	0.38
Hepatocyte Stability h/m (pred CL hep, ml/min/kg)	<8/<28	<8/58	<8/70	<8/67	<8/54	13/75	14/61

CBL-B E2-Ub assay bottom is ~10 nM; Probe Displacement assay bottom is ~1 nM

Piperidines and Pyrrolidines Optimally Fill the New Pocket

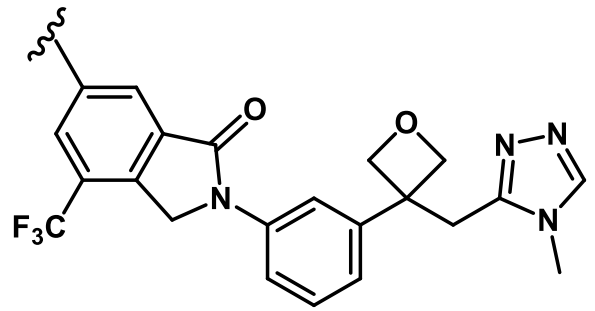

	H	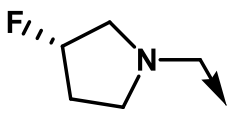	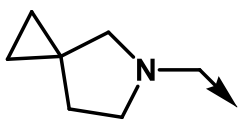	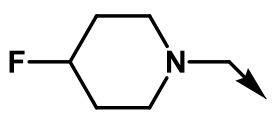	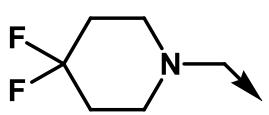	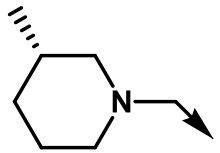	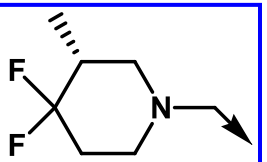
	NRX-25	NRX-26	NRX-27	NRX-28	NRX-29	NRX-30	NRX-31
CBL-B E2-Ub IC_{50} (nM)	150	5.1	5.1	4.8	6.2	8.8	4.9
TR-FRET Probe Displacement (nM)		9.1	4.2	4.7	8.6	2.0	1.6
T-cell IL-2 AUC		32.2	38	43.1	39	23.4	54
T-cell IL-2 2.5x (nM)	2500	72.1	6.4	12.8	17.6	6.3	0.38
Hepatocyte Stability h/m (pred CL hep, ml/min/kg)	<8/<28	<8/58	<8/70	<8/67	<8/54	13/75	14/61

CBL-B E2-Ub assay bottom is ~10 nM; Probe Displacement assay bottom is ~1 nM

Hypothesis: Slow Off-rate Drives T-cell Activity

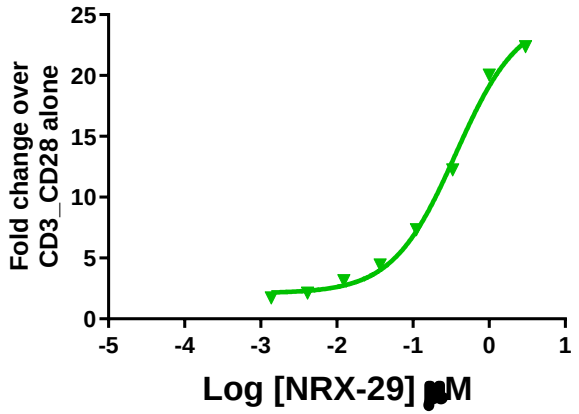

T-cell IL-2 AUC	39
T-cell IL-2 2.5x (nM)	17.6

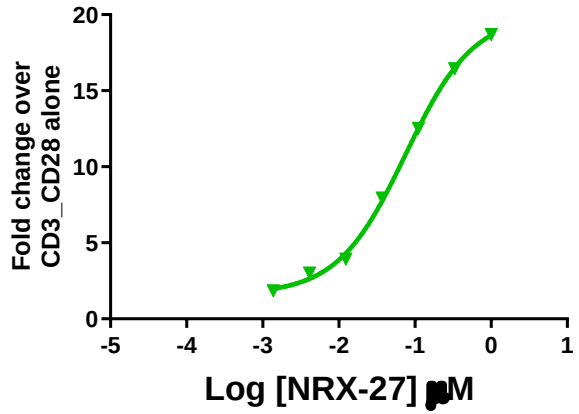

T-cell IL-2 AUC	38
T-cell IL-2 2.5x (nM)	6.4

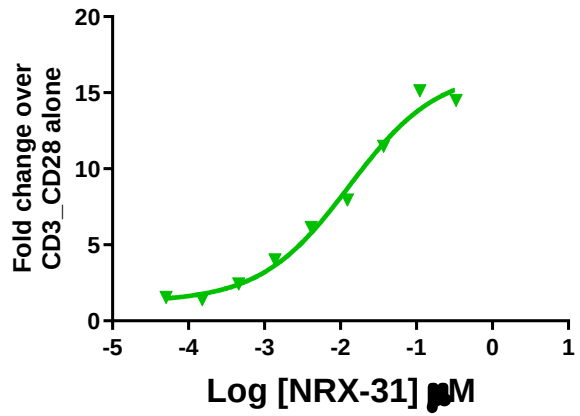

T-cell IL-2 AUC	54
T-cell IL-2 2.5x (nM)	0.38

Hypothesis: Slow Off-rate Drives T-cell Activity

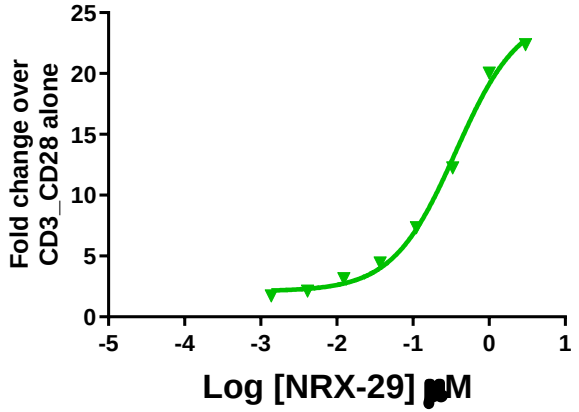

T-cell IL-2 AUC	39
T-cell IL-2 2.5x (nM)	17.6

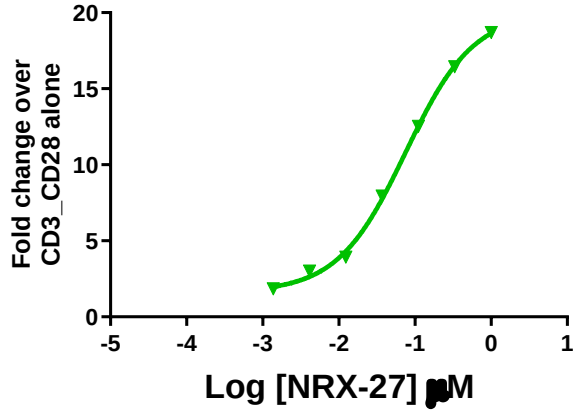

T-cell IL-2 AUC	38
T-cell IL-2 2.5x (nM)	6.4

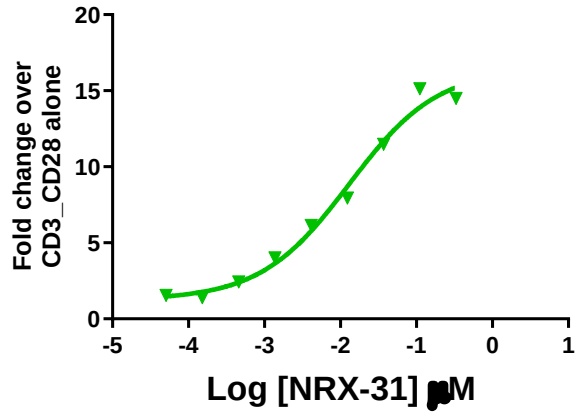

T-cell IL-2 AUC	54
T-cell IL-2 2.5x (nM)	0.38

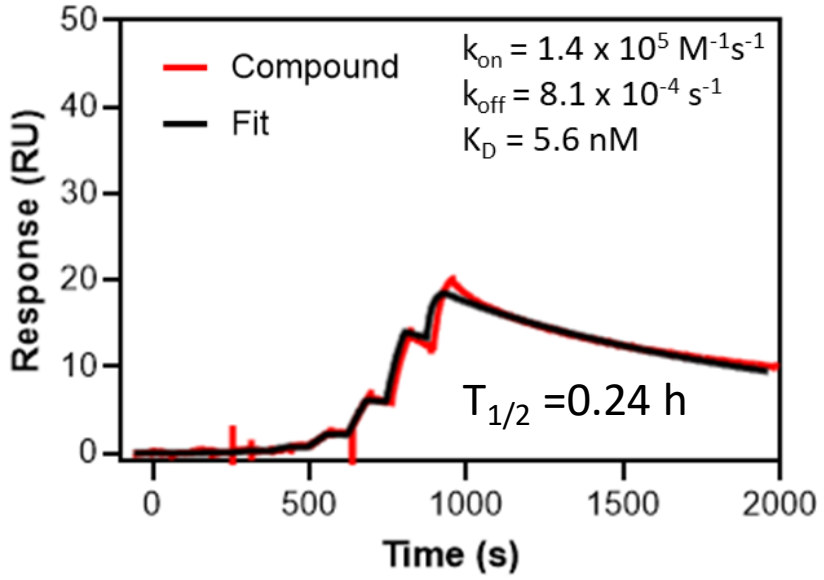

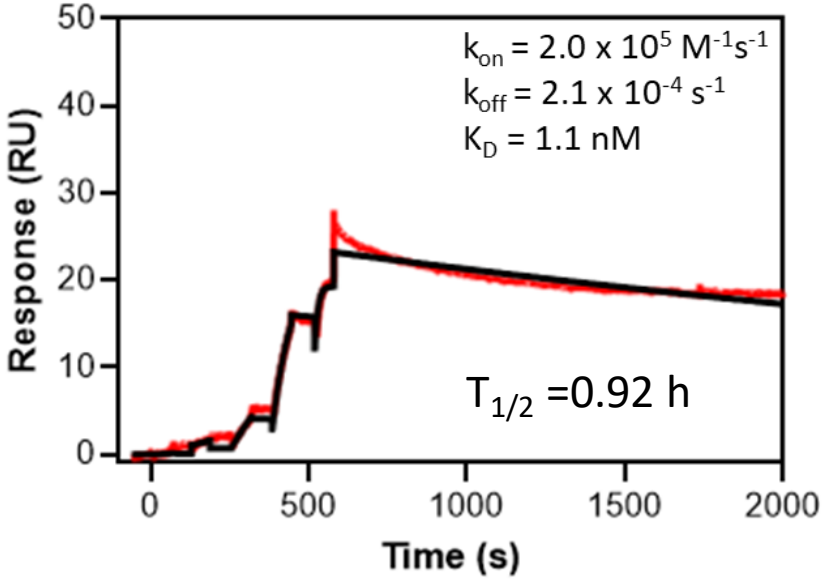

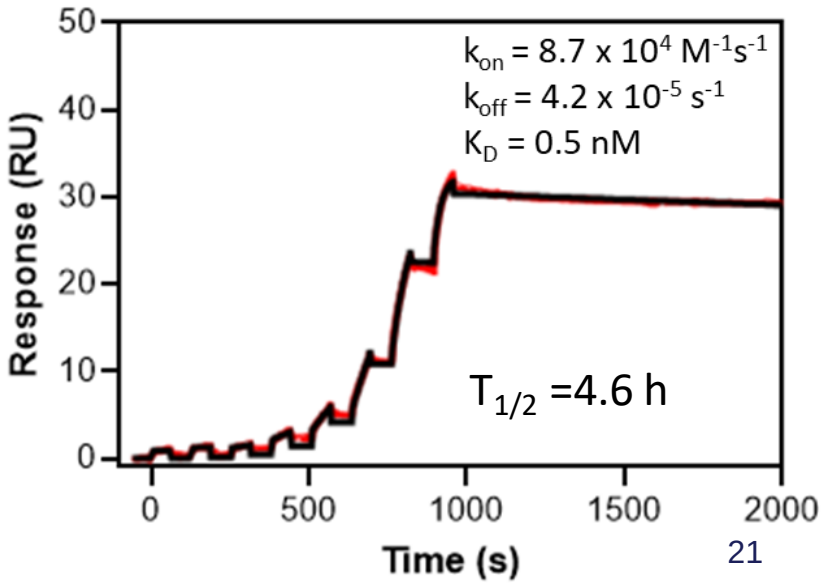

Structural Hypothesis for Slow Off-Rate

Overlay of crystal structures of 5 inhibitor (pink) structures with CBL-B that either do not fill or sub-optimally fill the second pocket (Cyan) shows a highly consistent protein structure

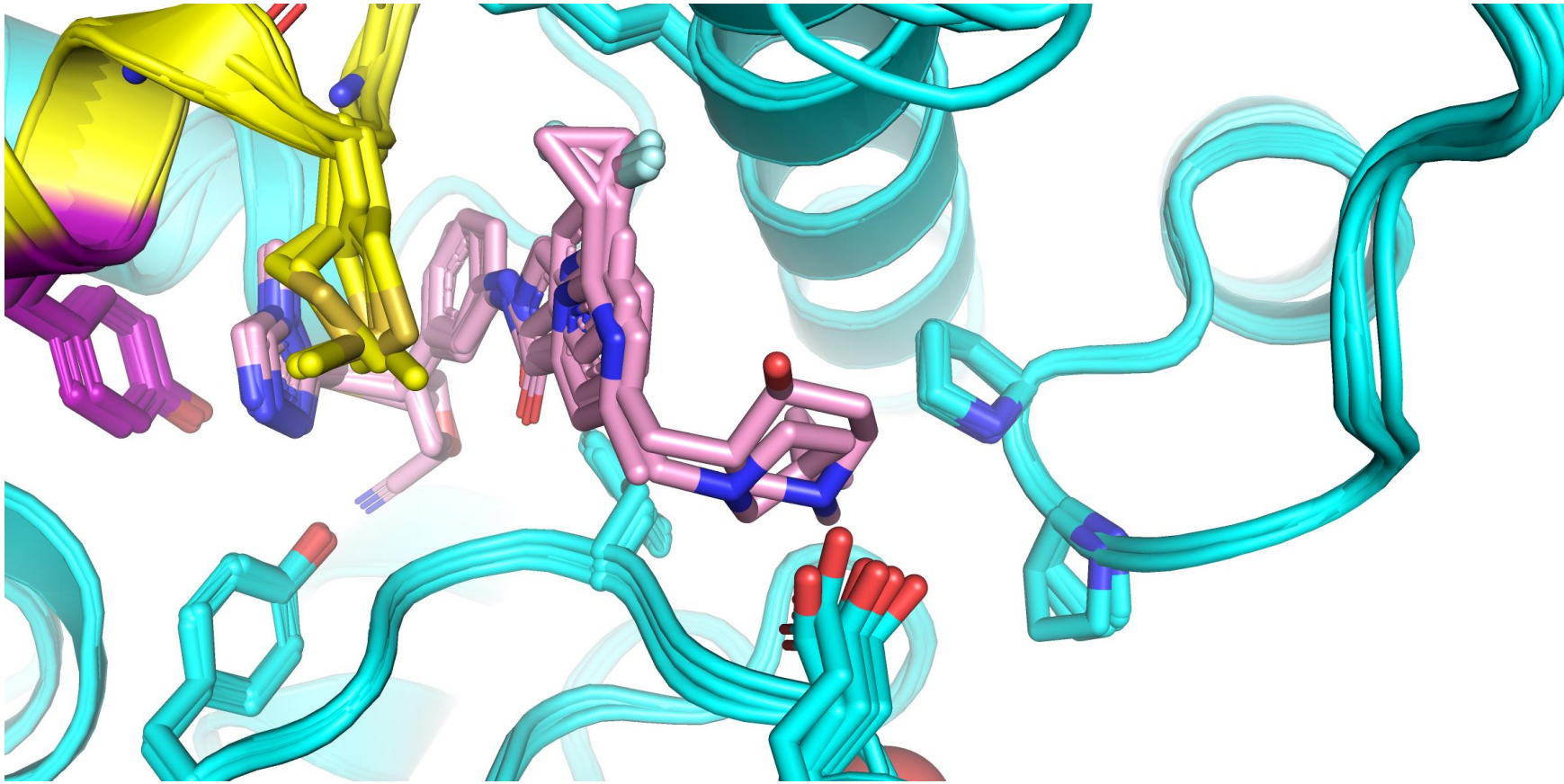

Structural Hypothesis for Slow Off-Rate

Overlay of crystal structures of 5 inhibitor (pink) structures with CBL-B that either do not fill or sub-optimally fill the second pocket (Cyan) shows a highly consistent protein structure

Overlay of 6 crystal structures of inhibitors with slightly larger substituents reveals a large movement in the pro-pro loop (Gold)

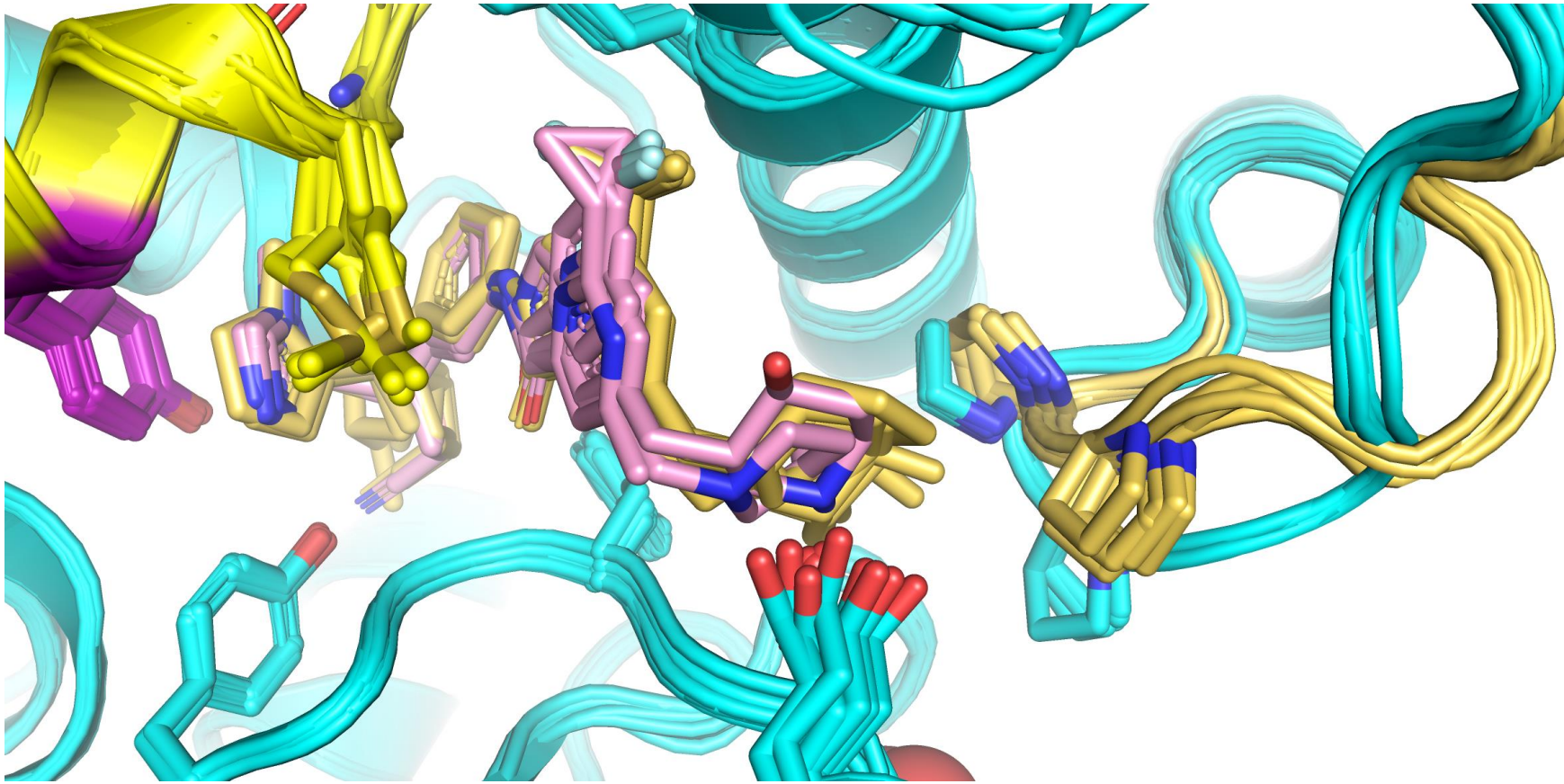

T-cell Activity Drives *in vivo* PD

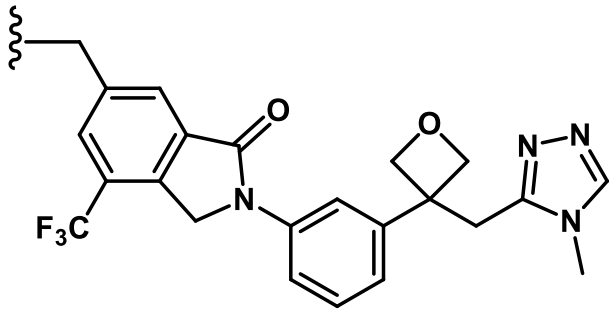

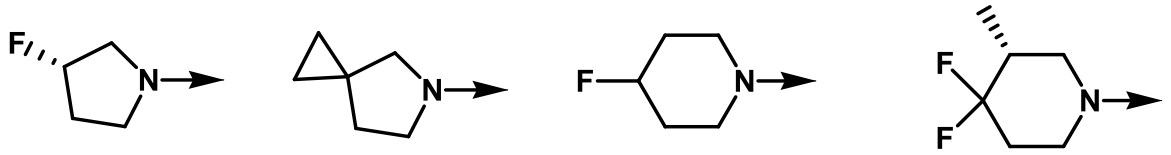

		NRX-26	NRX-27	NRX-28	NRX-31	
	T-cell IL-2 2.5x (nM)	72.1	6.4	12.8	0.38	
	Hepatocyte Stability h/m (pred CL hep, ml/min/kg)	<8/58	<8/70	<8/67	14/61	
Mouse PKPD	Dose mg/kg; freq	180/BID#	180/BID#	135/BID#	180/BID#	90/QD
	Free Conc 2h/7.5h (nM)	200/-	830/54	455/22	844/100	830/19
	Fold increase CD25+/CD4+ cells (24h)	1.3	2.0	1.6	3.6	2.2

#BID doses at T 0, 8h

Shortened Linkers Provide Improved Activity

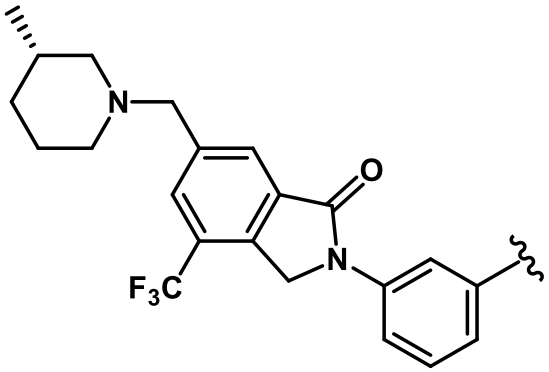

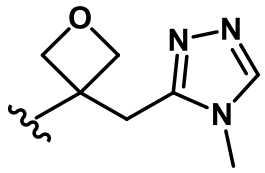

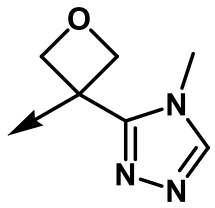

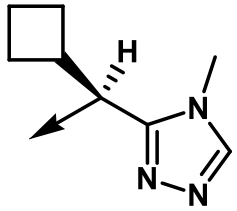

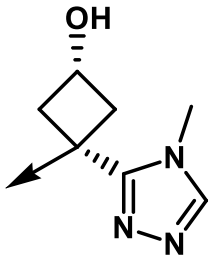

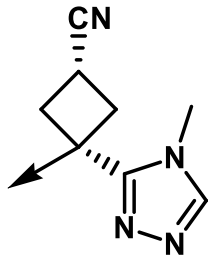

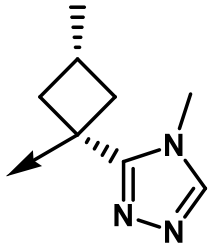

	NRX-30	NRX-32	NRX-33	NRX-34	NRX-35	NRX-36
CBL-B Probe Displacment-IC_{50} (nM)	2.0	65.1	0.47	2.7	2.5	0.46
T-cell IL-2 2.5x (nM)	6.3	-	0.057	4.89	1.79	0.054
Hepatocyte Stability h/m (pred CL hep, ml/min/kg)	13/75	<8/71	16/60	9/66	14/59	18/67

Shortened Linkers Provide Improved Activity

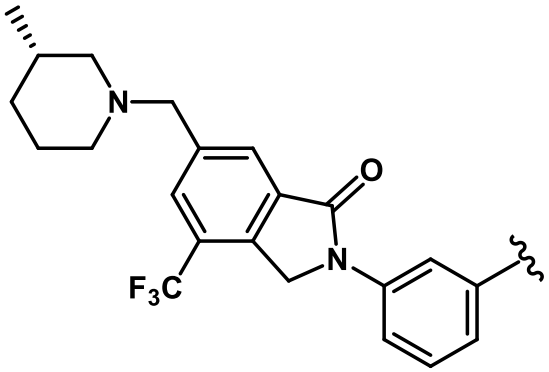
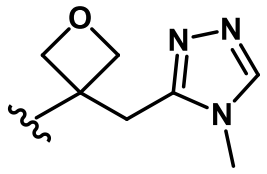
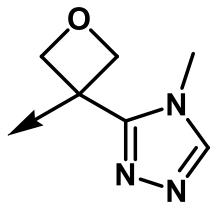
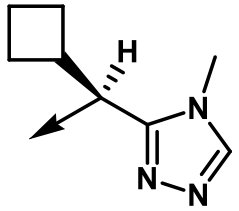
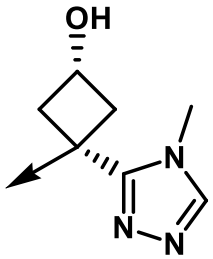
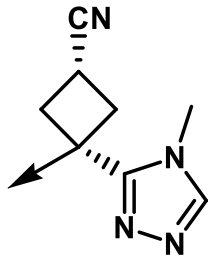
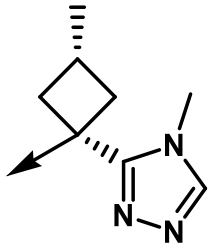

	NRX-30	NRX-32	NRX-33	NRX-34	NRX-35	NX-1607
CBL-B Probe Displacment-IC_{50} (nM)	2.0	65.1	0.47	2.7	2.5	0.46
T-cell IL-2 2.5x (nM)	6.3	-	0.057	4.89	1.79	0.054
Hepatocyte Stability h/m (pred CL hep, ml/min/kg)	13/75	<8/71	16/60	9/66	14/59	18/67
Mouse PKPD: Dose mg/kd; freq						90/QD / 45/BID#
Mouse PKPD: Free Conc 2h/7.5h (nM)						280/48 / 120/5
Mouse PKPD: Fold increase CD25+/CD4+ cells (24h)						2.6 / 4.4

#BID doses at T 0, 8h

Shortened Spacer Molecules Maintain Key Interactions

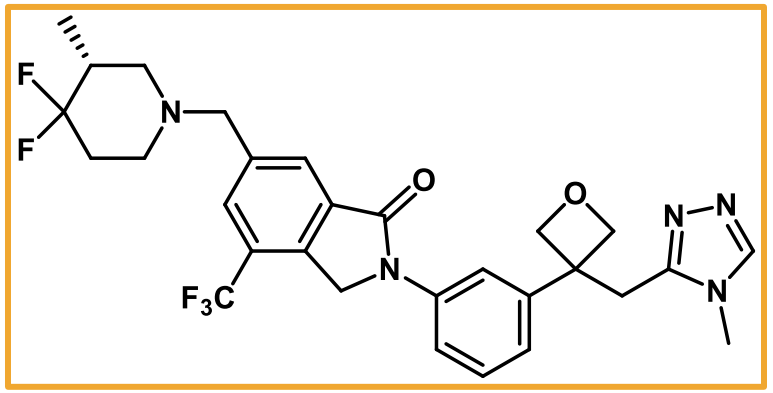

NRX-31

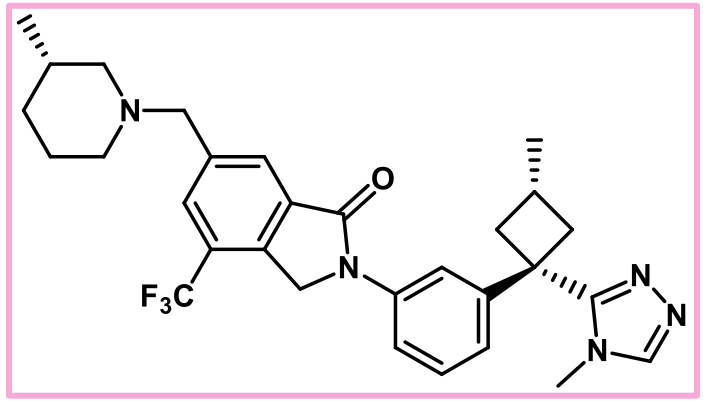

NX-1607

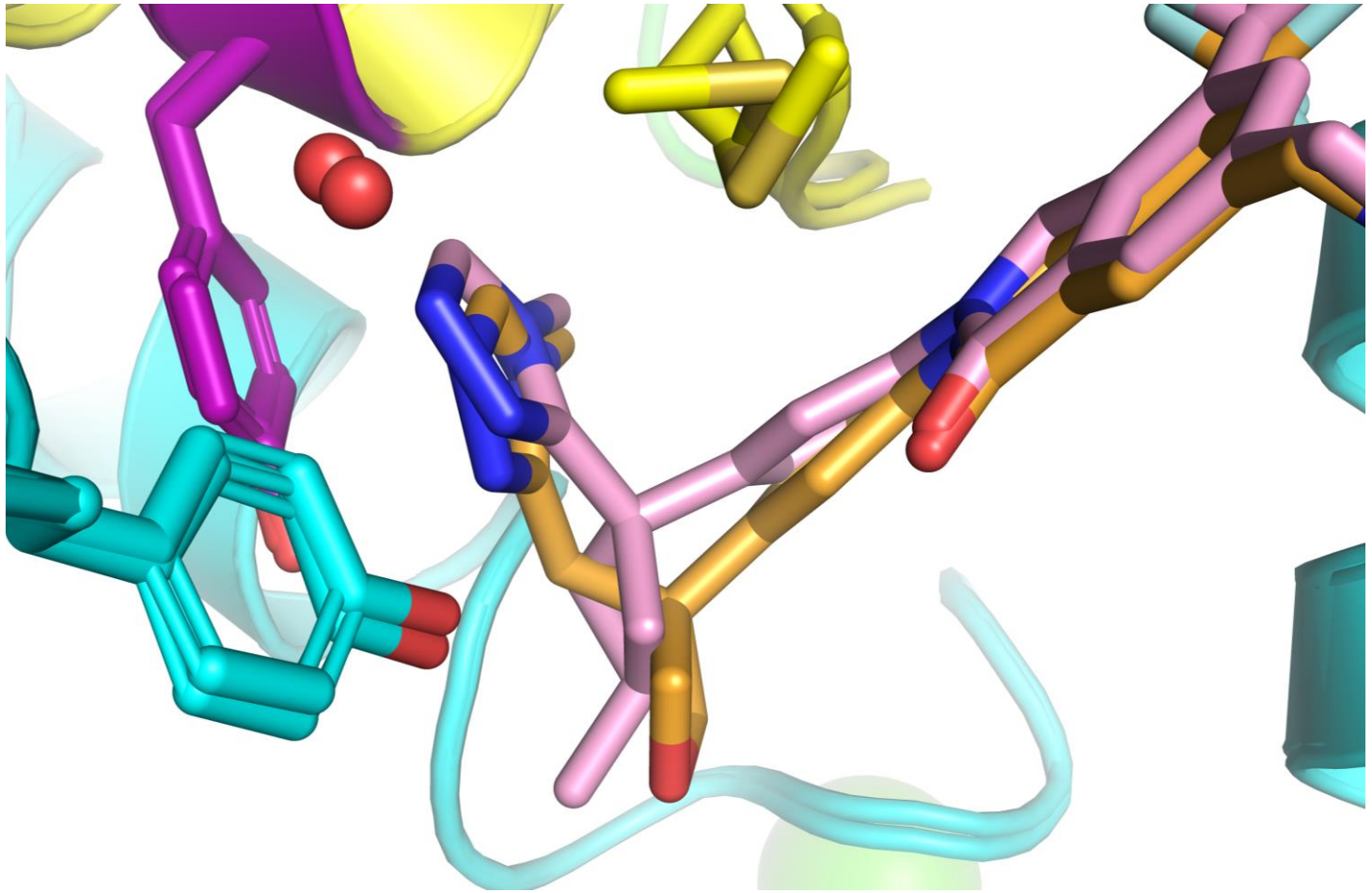

Over 10,000-fold Enzymatic Potency Improvement Achieved While Improving Molecular Properties

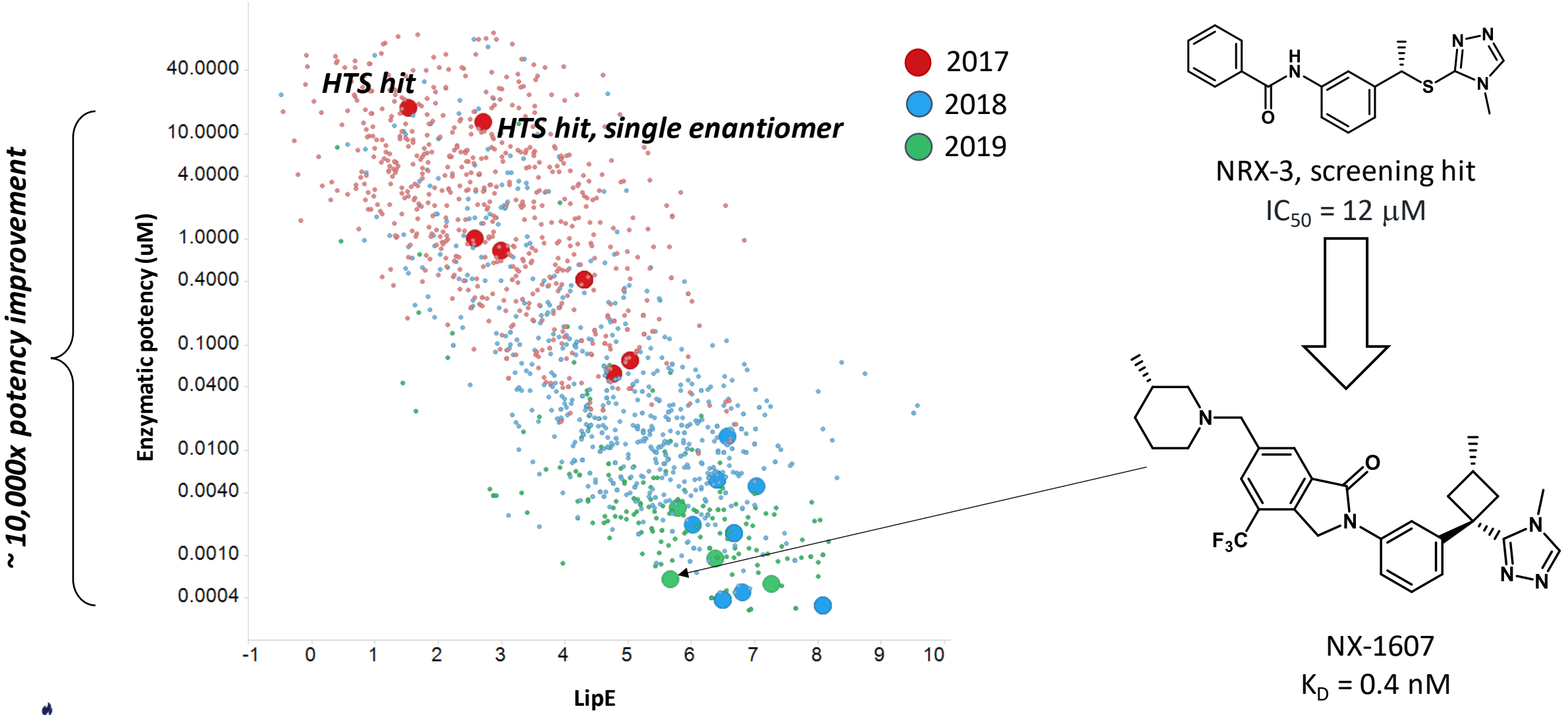

Single-Agent NX-1607 Induces Antitumor Response in Multiple Models

Colorectal (CT26)

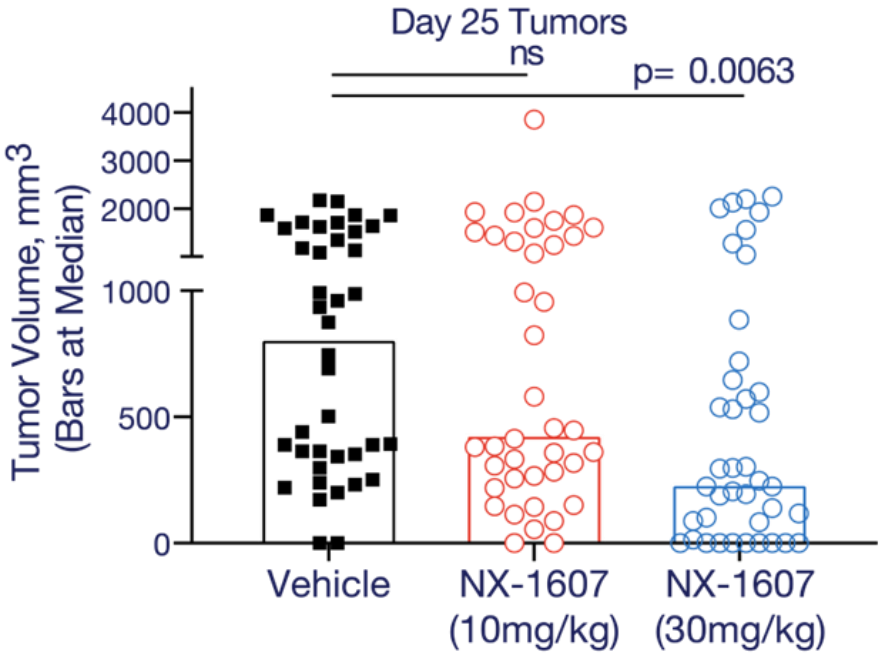

Triple-Negative Breast (4T1)

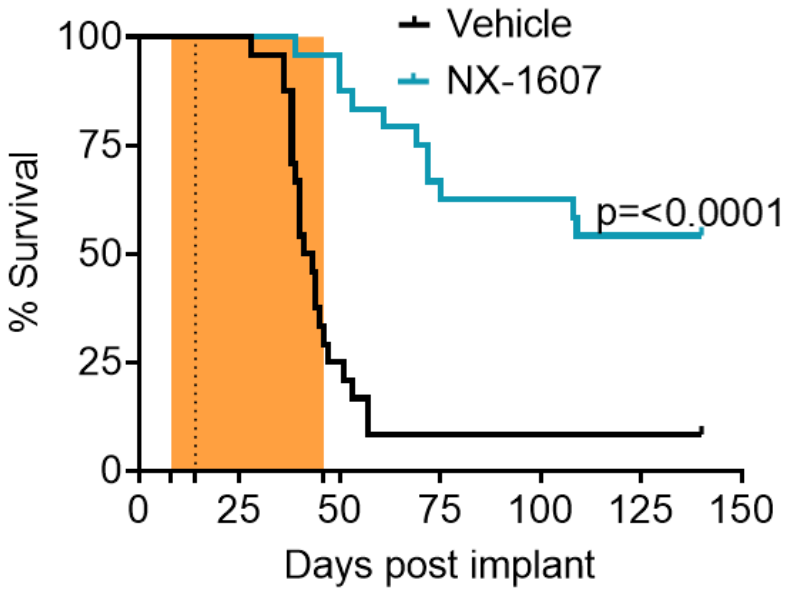

NX-1607 30 mg/kg QD day 7 to 46

B Cell Lymphoma (A20)

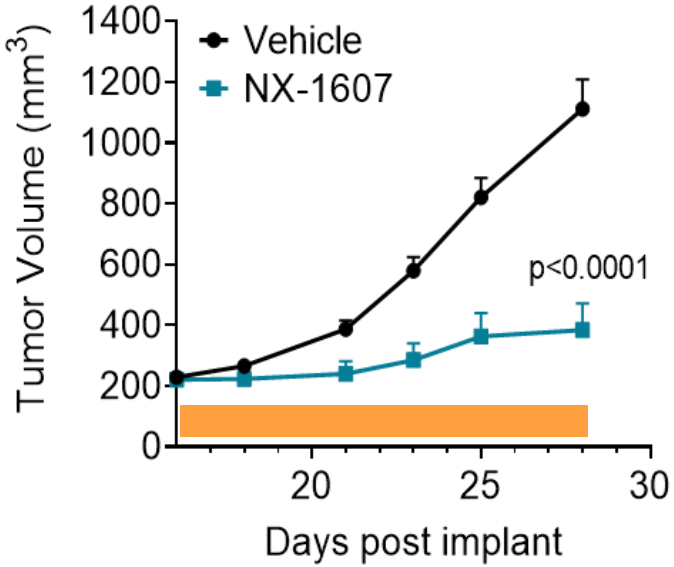

NX-1607 30 mg/kg QD 16 to 28

Shaded area indicates dosing period

NX-1607 and Anti-PD-1 Synergize to Enhance Survival in Multiple Models

Colorectal (CT26)

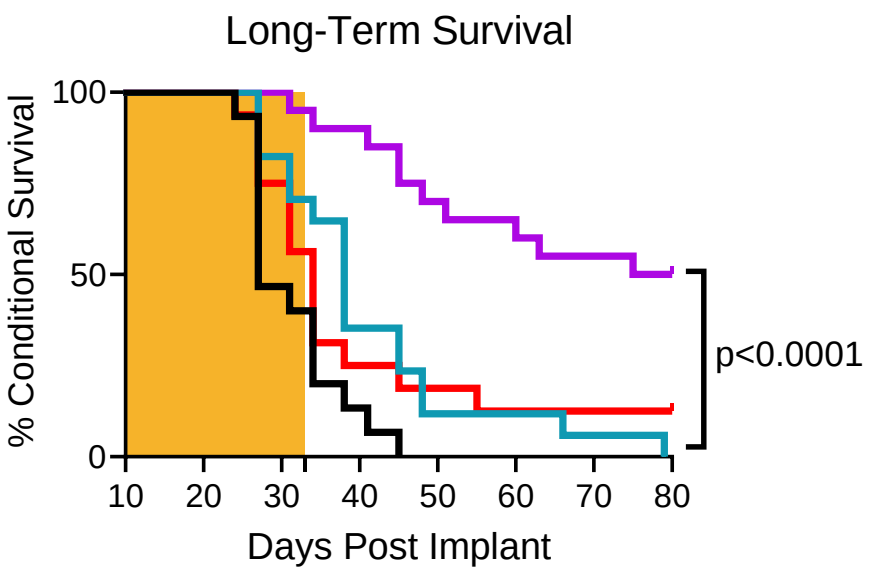

Colorectal (MC38)

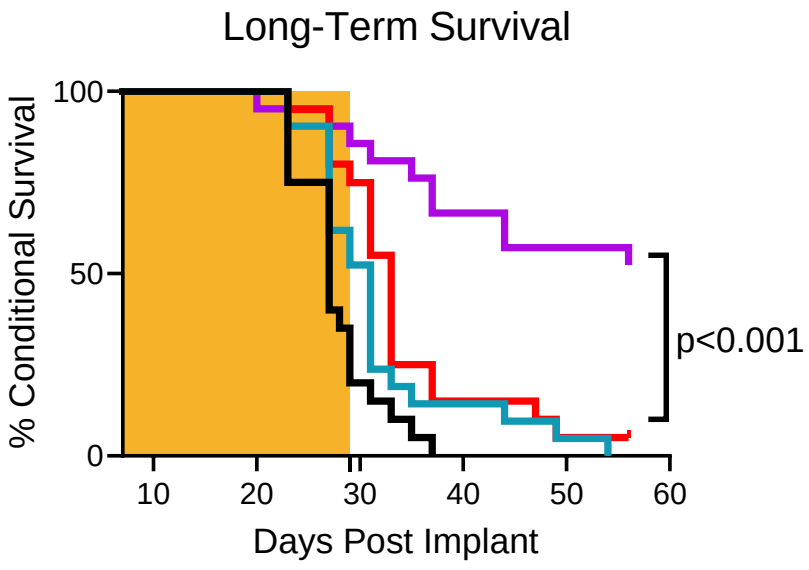

Triple-Negative Breast (4T1)

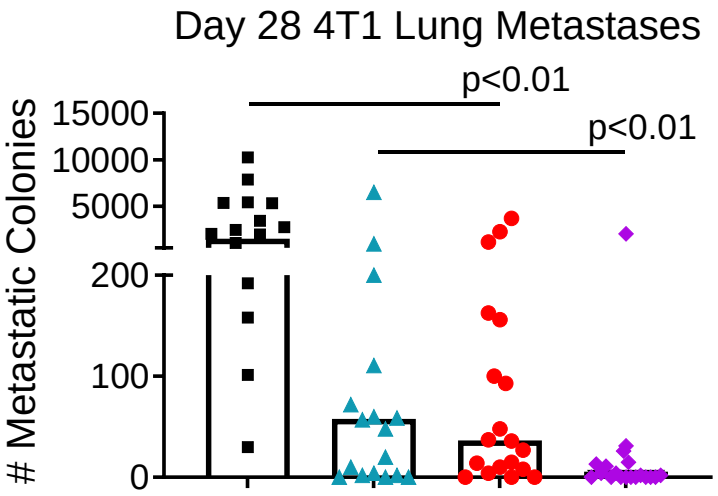

Vehicle NX-1607 anti-PD-1 NX-1607+anti-PD-1

Shaded area indicates dosing period: NX-1607 (30 mg/kg, PO daily) and anti-PD-1 (twice a week at 10 mg/kg)

NX-1607 Cross-Species PK

Cross-Species PK Findings

Parameters	Unit	Mouse	Rat	Dog	NHP
IV Dose	mg/kg	1	1	1	0.5
PO Dose	mg/kg	10	10	10	10
CL	mL/min/kg	59	40	16	27
	%Q	49	59	52	61
Vss	L/kg	1.4	3.2	2.0	2.8
IV $T_{1/2}$	h	0.33	1.4	1.7	1.6
F	%	25	0.23	48	7
PPB	% bound	97.3	96.2	94.6	96.2

Mean Plasma vs Time profiles for NX-1607 after 10 mg/kg PO Dose

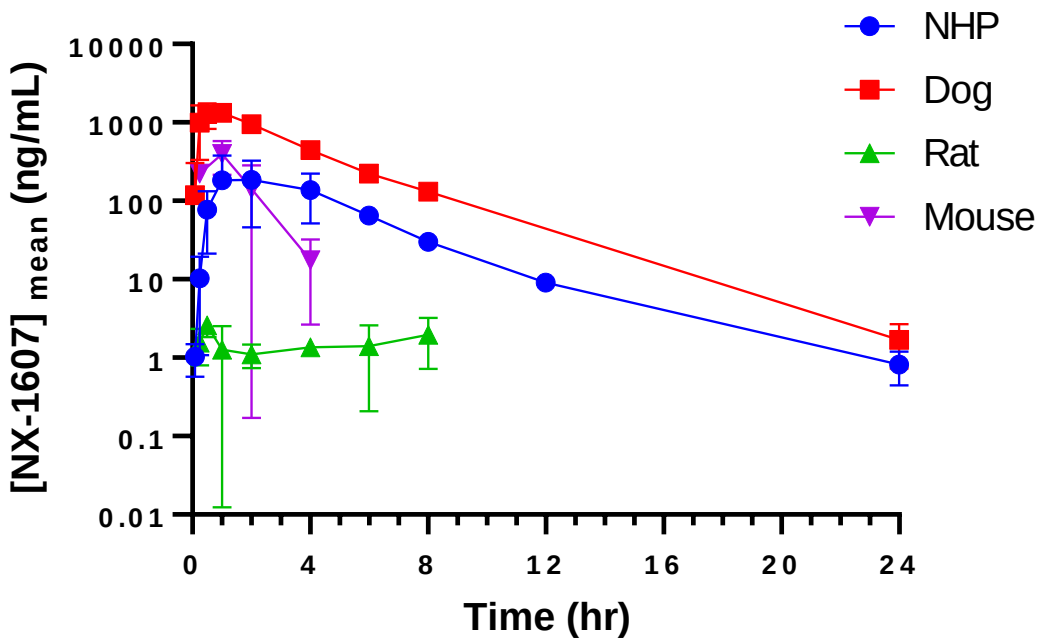

- NX-1607 has CL rates ~50% of LBF across preclinical species
- Is moderately bound to plasma
- Has moderate to good oral bioavailability (except in rat)

NX-1607 Displays Favorable *in vitro* Safety Profile

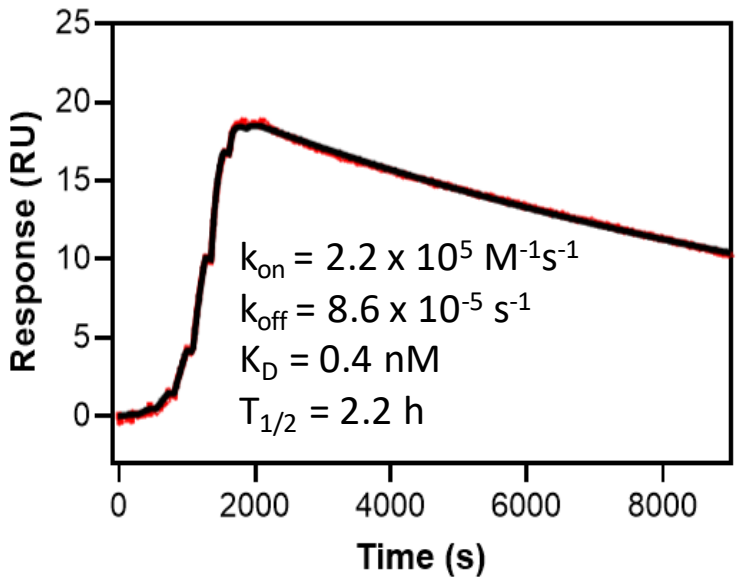

SPR sensogram for the binding kinetics and affinity measurements of NX-1607 to CBL-B.

The dark red curves are fitted curves generated from a 1:1 binding model.

NX-1607 Properties	
Parameter	Value
mw	537.6 amu
pKa/Log$D_{7.4}$	8.3/3.5
Solubility (PBS, pH=7.4)	230 uM
K_D CBL-B (nM) spr	0.4
K_D C-CBL (nM) spr	1.43
CACO Permeability A-B(10^{-6} cm/sec) B-A Ratio	 18.3 2.3
hPPB	97.1
CYP (%I @ 10 uM) 1A2/2B6/2C9/2C19/2D6/	 14/18/48/42/28
CYP3A4 IC_{50}, uM Tst/mid	 3.9/6.0
GSH trapping/TDI	Neg
Ames/MNT (+/- S9)	Neg

Concentration-response relationship of NX-1607 on hERG current

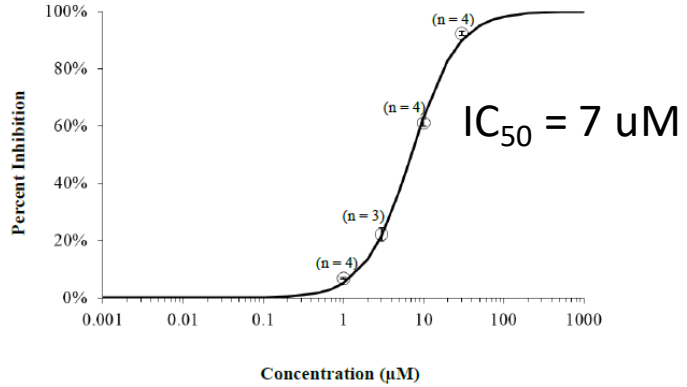

- Measured IC_{50} (CEREP&hERG) values are >100X predicted efficacious free drug concentration in patients
- 28-day Tox studies in rat and NHP were supportive of advancement to clinical testing.

NX-1607-101 Interim Clinical PK Results Suggest Linear PK

Preliminary PK data suggest NX-1607 has dose-proportional exposures and a mean half-life of 6 to 8 hours at doses ranging from 5 to 50 mg (NCT05107674).

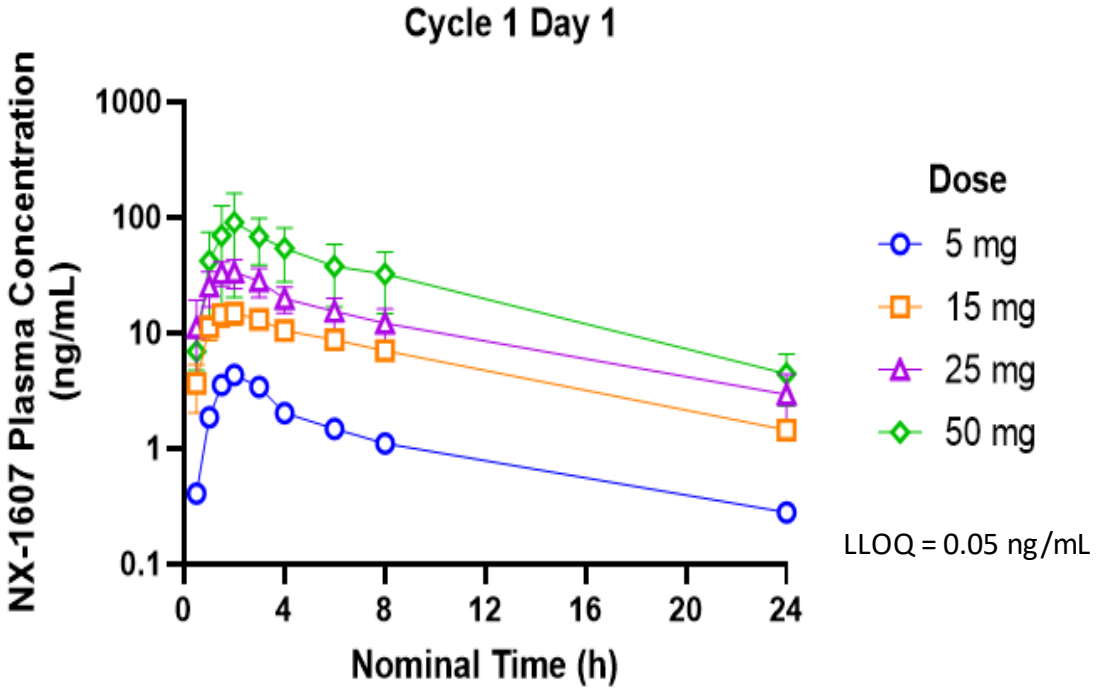

Dose	Cycle 1 Day 1			
	C_{max} (ng/mL)	$AUC_{0\text{-last}}$ (h*ng/mL)	T_{max} (h)	$t_{1/2}$ (h)
5 mg (n=1)	4.35	26.2	2.0	7.72
15 mg (n=9)	16.2 (38.5)	129 (33.4)	2.0 (1.5 - 6.0)	7.14 (19.8)
25 mg (n=6)	30.1 (109)	201 (103)	1.5 (1.0 - 3.0)	6.82 (27.5)
50 mg (n=2)	79.2 (134)	502 (113)	2.5 (2.0 - 3.0)	5.88 (7.7)

C_{max} and $AUC_{0\text{-last}}$ are presented as geometric mean (geometric %CV); T_{max} is presented as median (range); $t_{1/2}$ is presented as mean (%CV)

Dose-proportional increases in PK/PD observed in NX-1607-101 clinical trial are consistent with the potent anti-tumor activity seen in preclinical mouse models:

Whelan, S., et al. (2022) Society for Immunotherapy of Cancer (SITC) 2022, Boston, MA.

Summary

- A novel HTS assay was developed to screen for multiple modes of CBL-B inhibition
- A singleton hit was confirmed to be an intramolecular glue, stabilizing the closed, inactive state of the ligase
- The compound series was optimized for T-cell activation leveraging *in vitro* and *in vivo* assays
- NX-1607:
  - Single-agent efficacy in multiple mouse tumor models
  - Synergizes with anti-PD1
  - Pre-clinical safety profile supportive of clinical study
  - Currently in a Phase 1 clinical trial (NCT05107674)
  - Linear PK in patients at doses from 5 to 50 mg